Lecture notes on

Nanomagnetism

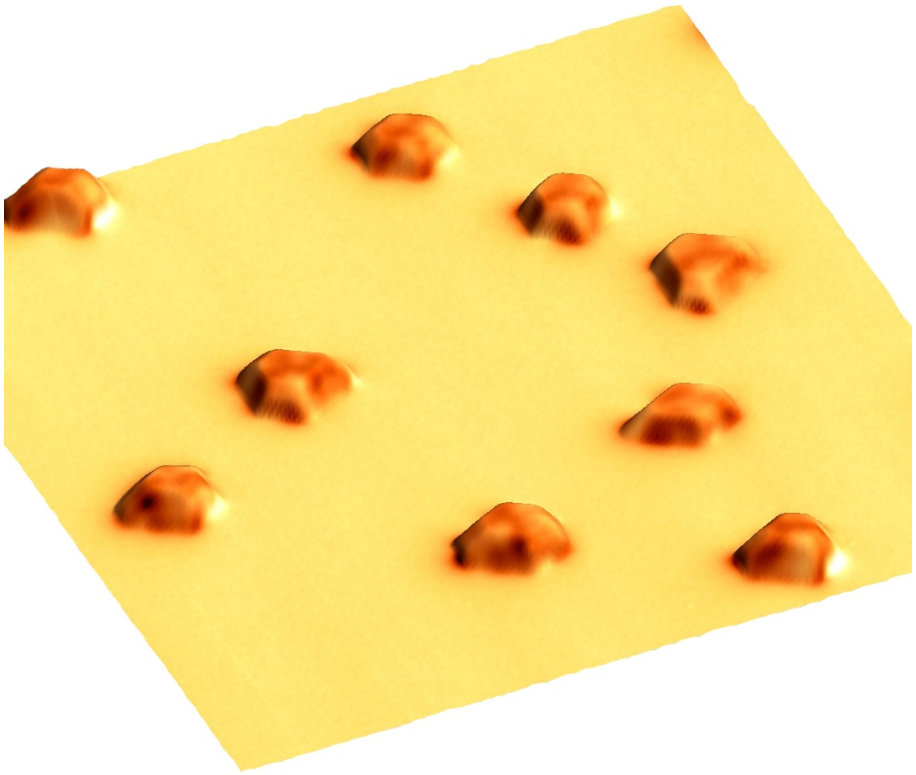

Olivier Fruchart
Institut Néel (CNRS & UJF) – Grenoble

Version : December 2, 2011
Olivier.Fruchart-at-grenoble.cnrs.fr
http://perso.neel.cnrs.fr/olivier.fruchart/

Contents

Introduction

Content

This manuscript is based on series of lectures about *Nanomagnetism*. Parts have been given at the European School on Magnetism, at the École Doctorale de Physique de Grenoble, or in Master lectures at the Cadi Ayyad University in Marrakech.

Nanomagnetism may be defined as the branch of magnetism dealing with low-dimension systems and/or systems with small dimensions. Such systems may display behaviors different from those in the bulk, pertaining to magnetic ordering, magnetic domains, magnetization reversal etc. These notes are mainly devoted to these aspects, with an emphasis on magnetic domains and magnetization reversal.

Spintronics, *i.e.* the physics linking magnetism and electrical transport such as magnetoresistance, is only partly and phenomenologically mentioned here. We will consider those cases where spin-polarized currents influence magnetism, however not when magnetism influences the electronic transport.

This manuscript is only an introduction to Nanomagnetism, and also sticking to a classical and phenomenological descriptions of magnetism. It targets beginners in the field, who need to use basics of Nanomagnetism in their research. Thus the explanations aim at remaining understandable by a large scope of physicists, while staying close to the state-of-the art for the most advanced or recent topics.

Finally, **these notes are never intended to be in a final form, and are thus by nature imperfect. The reader should not hesitate to report errors or make suggestions about topics to improve or extend further**. A consequence is that it is probably unwise to print this document. Its use as an electronic file is anyhow preferable to benefit from the included links within the file. At present only chapters I and II are more or less completed.

Notations

As a general rule, the following typographic rules will be applied to variables:

Characters

- A microscopic extensive or intensive quantity appears as slanted uppercase or Greek letter, such as H for the magnitude of magnetic field, E for a density of energy expressed in J/m^3, ρ for a density.
- An extensive quantity integrated over an entire system appears as handwritten uppercase. A density of energy E integrated over space will thus be written $\mathcal{E}$, and expressed in J.

- A microscopic quantity expressed in a dimensionless system appears as a handwritten lowercase, such as e for an energy or h for a magnetic field normalized to a reference value. Greek letters will be used for dimensionless versions of integrated quantities, such as ϵ for a total energy.
- Lengths and angles will appear as lower case roman or Greek letters, such as x for a length or α for an angle. If needed, a specific notation is introduced for dimensionless lengths.
- A vector appears as bold upright, with no arrow. Vectors may be lowercase, uppercase, handwritten or Greek, consistently with the above rules. We will thus write $\mathbf{H}$ for a magnetic field, $\mathbf{h}$ its dimensionless counterpart, $\mathbf{k}$ a unit vector along direction z, $\boldsymbol{\mathcal{M}}$ or $\boldsymbol{\mu}$ a magnetic moment.

Mathematics

- The cross product of two vectors $\mathbf{A}$ and $\mathbf{B}$ will be written $\mathbf{A} \times \mathbf{B}$.
- The following shortcut may be used: $\partial_x \theta$ for $\partial\theta/\partial x$, or $\partial^n_{x^n}\theta$ for $\frac{\partial^n \theta}{\partial x^n}$.
- The elementary integration volume integration may be written $\mathrm{d}^3 r$ or $\mathrm{d}\tau$, and the surface on: $\mathrm{d}^2 r$ or $\mathrm{d}S$.

Units

- The International system of units (SI) will be used for numerical values.
- B will be called magnetic induction, H magnetic field, and M magnetization. We will often use the name *magnetic field* in place of B when no confusion exists, *i.e.* in the absence of magnetization (in vacuum). This is a shortcut for B/μ_0, to be expressed in Teslas.

Special formatting

Special formatting is used to draw the attention of the reader at certains aspects, as illustrated below.

Words highlighted like this are of special importance, either in the local context, or when they are important concepts introduced for the first time.

The hand sign will be associated with hand-wavy arguments and take-away messages.

The slippery sign will be associated with misleading aspects and fine points.

Chapter I

Setting the ground for nanomagnetism

Overview

A thorough introduction to Magnetism[1, 2, 3] and Micromagnetism and Nanomagnetism[4, 5, 6, 7] may be sought in dedicated books. This chapter only serves as an introduction to the lecture, and it is not comprehensive. We only provide general reminders about magnetism, micromagnetism, and of some characterization techniques useful for magnetic films and nanostructures.

1 Magnetic fields and magnetic materials

1.1 Magnetic fields

Electromagnetism is described by the four Maxwell equations. Let us consider the simple case of stationary equations. Magnetic induction $\mathbf{B}$ then obeys two equations:

$$\mathbf{curl}\,\mathbf{B} = \mu_0\,\mathbf{j} \tag{I.1}$$

$$\mathrm{div}\,\mathbf{B} = 0 \tag{I.2}$$

$\mathbf{j}$ being a volume density of electrical current. $\mathbf{j}$ appears as a source of induction loops, similar to electrostatics where the density of electric charge ρ is the source of radial electric field $\mathbf{E}$. Let us first consider the simplest case for an electric current, that of an infinite linear wire with total current I. We shall use cylindrical coordinates. Any plane comprising the wire is a symmetry element for the current and thus an antisymmetric element for the induced induction (see above equations), which thus is purely orthoradial and described by the component B_θ only. In addition the system is invariant by rotation around and translation along the wire, so that B_θ depends neither on θ nor z, however solely on the distance r to the wire. Applying Stokes theorem to an orthoradial loop with radius r (Figure I.1) readily leads to:

$$B_\theta(r) = \frac{\mu_0 I}{2\pi r} \tag{I.3}$$

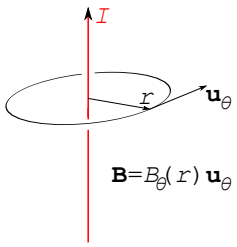

Figure I.1: So-called Oersted magnetic induction$B$, arising from an infinite and linear wire with an electrical current I.

This is the so-called Oersted induction or Oersted field, named after its discovery in 1820 by Hans-Christian OERSTED. This discovery was the first evidence of the connection of electricity and magnetism, and is therefore a foundation for the development of electromagnetism. Notice the variation with $1/r$. Let us consider an order of magnitude for daily life figures. For $I = 1\,\mathrm{A}$ and $r = 10^{-2}\,\mathrm{m}$ we find $B = 2 \times 10^{-5}\,\mathrm{T}$. This magnitude is comparable to the earth magnetic field, around $50\,\mu\mathrm{T}$. It is weak compared to fields arising from permanent magnets or dedicated electromagnets and superconducting magnets.

We may argue that there exists no infinite line of current. The Biot and Savart law describes instead the elementary contribution to induction $\delta\mathbf{B}$ at point P, arising from an elementary part of wire $\delta\boldsymbol{\ell}$ at point Q with a current I:

$$\delta\mathbf{B}(P) = \frac{\mu_0 I\,\delta\boldsymbol{\ell} \times \mathbf{QP}}{4\pi QP^3} \tag{I.4}$$

Notice this time the variation as $1/r^2$. This can be understood qualitatively as a macroscopic (infinite) line is the addition (mathematically, the integral) of elementary segments, and we have $\int 1/r^2 = 1/r$. It may also be argued that there exists no elementary segments of current for conducting wirings, however only closed circuits (loops), with a uniform current I along its length. When viewed as a distance far compared to its dimensions, a loop of current may be considered as a pinpoint magnetic dipole $\boldsymbol{\mu}$. This object is an example of a magnetic moment. For a planar loop $\boldsymbol{\mu} = I\mathbf{S}$ where $\mathbf{S}$ is the surface vector normal to the plane of the loop, oriented accordingly with the electrical current. Here it appears clearly that the SI unit for a magnetic moment is $\mathrm{A.m^2}$. The expansion of the Biot and Savart law leads to the induction arising from a dipole at long distance $\mathbf{r}$:

$$\mathbf{B}(\mathbf{r}) = \frac{\mu_0}{4\pi r^3}\left[3\frac{(\boldsymbol{\mu}.\mathbf{r})\mathbf{r}}{r^2} - \boldsymbol{\mu}\right]. \tag{I.5}$$

Let us note now the variation with $1/r^3$. This may be understood as the first derivative of the variation like $1/r^2$ arising from an elementary segment, due to nearby regions run by opposite vectorial currents j (*e.g.* the opposite parts of a loop).

Table I.1 summarizes the three cases described above.

Table I.1: Long-distance decay of induction arising from various types of current distributions

Case	Decay
Infinite line of current	$1/r$
Elementary segment	$1/r^2$
Current loop (magnetic dipole)	$1/r^3$

Table I.2: Main features of a few important ferromagnetic materials: Ordering (Curie) temperature T_C, spontaneous magnetization M_s and a magnetocristalline anisotropy constant K at 300 K (The symmetry of the materials, and hence the order of the anisotropy constants provided, is not discussed here)

Material	T_C (K)	M_s (kA/m)	$\mu_0 M_s$ (T)	K (kJ/m^3)
Fe	1043	1730	2.174	48
Co	1394	1420	1.784	530
Ni	631	490	0.616	-4.5
Fe_30_4	858	480	0.603	-13
$BaFe_{12}O_{19}$	723	382	0.480	250
$Nd_2Fe_{14}B$	585	1280	1.608	4900
$SmCo_5$	995	907	1.140	17000
Sm_2Co_{17}	1190	995	1.250	3300
FePt $L1_0$	750	1140	1.433	6600
CoPt $L1_0$	840	796	1.000	4900
Co_3Pt	1100	1100	1.382	2000

1.2 Magnetic materials

A magnetic material is a body which displays a magnetization $\mathbf{M}(\mathbf{r})$, *i.e.* a volume density of magnetic moments. The SI unit for magnetization therefore appears naturally A.m^2/m^3, thus A/m[I.1]. In any material some magnetization may be induced under the application of an external magnetic field $\mathbf{H}$. We define the magnetic susceptibility χ with $\mathbf{M} = \chi\mathbf{H}$. This polarization phenomenon is named diamagnetism for $\chi < 0$ and paramagnetism for $\chi > 0$.

Diamagnetism arises from a Lenz-like law at the microscopic level (electronic orbitals), and is present in all materials. χ_{dia} is constant with temperature and its value is material-dependent, however roughly of the order of 10^{-5}. Peak values are found for Bi ($\chi = -1.66 \times 10^{-4}$) and graphite along the c axis ($\chi \approx -4 \times 10^{-4}$). Such peculiarities may be explained by the low effective mass of the charge carriers

[I.1] We shall always use strictly the names magnetic moment and magnetization. Experimentally some techniques provide direct or indirect access to magnetic moments (*e.g.* an extraction magnetometer, a SQUID, magnetic force microscopy), other provide a m ore natural access to magnetization, often through data analysis (*e.g.* magnetic dichroism of X-rays, electronic or nuclear resonance).

involved.

Paramagnetism arises from partially-filled orbitals, either forming bands or localized. The former case is called Pauli paramagnetism. χ is then temperature-independent and rather weak, again of the order of 10^{-5}. The later case is called Curie paramagnetism, and χ scales with $1/T$. A useful order of magnitude in Curie paramagnetism to keep in mind is that a moment of $1\,\mu_B$ gets polarized at 1 K under an induction of 1 T.

Only certain materials give rise to paramagnetism, in particular metals or insulators with localized moments. Then diamagnetism and paramagnetism add up, which may give give to an overall paramagnetic of diamagnetic response.

Finally, in certain materials microscopic magnetic moments are coupled through a so-called exchange interaction, leading to the phenomenon of magnetic ordering at finite temperature and zero field. For a first approach magnetic ordering may be described in mean field theory modeling a molecular field, as we will detail for low dimension systems in Chapter II. The main types of magnetic ordering are:

- Ferromagnetism, characterized by a positive exchange interaction, end favoring the parallel alignement of microscopic moments. This results in the occurrence of a spontaneous magnetization M_s[I.2]. In common cases M_s is of the order of 10^6 A/m, which is very large compared to magnetization arising from paramagnetism or diamagnetism. The ordering occurs only at and below a temperature called the Curie temperature, written T_C. The only three pure elements ferromagnetic at room temperature are the 3d metals Fe, Ni and Co (Table I.2).

- Antiferromagnetism results from a negative exchange energy, favoring the antiparallel alignement of neighboring moments[I.3] leading to a zero net magnetization M_s at the macroscopic scale. The ordering temperature is in that case called the Néel temperature, and is written T_N.

- Ferrimagnetism arises in the case of negative exchange coupling between moments of different magnitude, because located each on a different sublattice[I.4], leading to a non-zero net magnetization. The ordering temperature is again called Curie temperature.

Let us consider the simple case of a body with uniform magnetization, for example a spontaneous magnetization $\mathbf{M}_s = M_s\mathbf{k}$ (Figure I.2). It is readily seen that the equivalent current loops modeling the microscopic moments cancel each other for neighboring loops: only currents at the perimeter remain. The body may thus be modeled as a volume whose surface carries an areal density of electrical current, whose magnitude projected along $\mathbf{k}$ is M_s. This highlights a practical interpretation of the magnitude of magnetization expressed in A/m.

Let us stress a fundamental quantitative difference with Oersted fields. We consider again a metallic wire carrying a current of 1 A. For a cross-section of $1\,\text{mm}^2$ a single wiring has 1000 turns/m. The equivalent magnetization would be 10^3 A/m, which is three orders of magnitude smaller than M_s of usual ferromagnetic

[I.2] The s in M_s is confusing between the meanings of spontaneous and saturation. We will discuss this fine point in the next paragraph

[I.3] More complexe arrangements, non-colinear like spiraling, exist like in the case of Cr

[I.4] Similarly to antiferromagnetism, more complex arrangements may be found

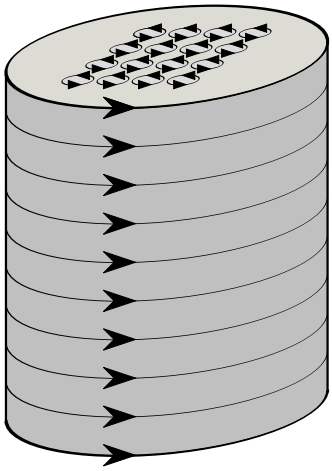

Figure I.2: Amperian description of a ferro (or ferri-)magnetic material: microscopic currents cancel each other between neighboring regions, except at the perimeter of the body.

materials. Thus a significant induction may easily be obtained from the stray field of a permanent magnet, of the order of $\mu_0 M_s \approx 1\,\mathrm{T}$. It is possible to reach magnitude of induction of several Teslas with wirings, however with special designs: large and thick water-cooled coils to increase the current density and total value, or use superconducting wires however requiring their use at low temperature, or use pulsed currents with high values, this time requiring small dimensions to minimize self-inductance.

Let us finally recall the relationship between induction, magnetic field and magnetization:

$$\mathbf{B} = \mu_0(\mathbf{H} + \mathbf{M}) \tag{I.6}$$

This relationship may be proven starting from Maxwell's equations, considering as two different entities the free electrical charges, and the so-called bound charges giving rise to the magnetization $\mathbf{M}$.

1.3 Magnetic materials under field – The hysteresis loop

Let us consider a system mechanically fixed in space, subjected to an applied magnetic field $\mathbf{H}$. This field gives rise to a Zeeman energy, written $E_Z = -\mu_0 \mathbf{M}_s.\mathbf{H}$ for a volume density, or $\mathcal{E}_Z = -\mu_0 \boldsymbol{\mu}.\mathbf{H}$ for the energy of a magnetic moment. The consequence is that magnetization will tend to align itself along $\mathbf{H}$, which shall be attained for a sufficient magnitude of $\mathbf{H}$. This process is called a magnetization process, or magnetization reversal. The quantity considered or measured may be a moment or magnetization, the former in magnetometers and the latter in some magnetic microscopes or in the Extraordinary Hall Effect, for example. It is often displayed, in models or as the result of measurements, as a hysteresis loop, also called magnetization loop or magnetization curve. The horizontal axis is often H or $\mu_0 H$, while the y axis is the projection of the considered quantity along the direction of $\mathbf{H}$ [*e.g.*: $(\mathbf{M}.\mathbf{H})/H$].

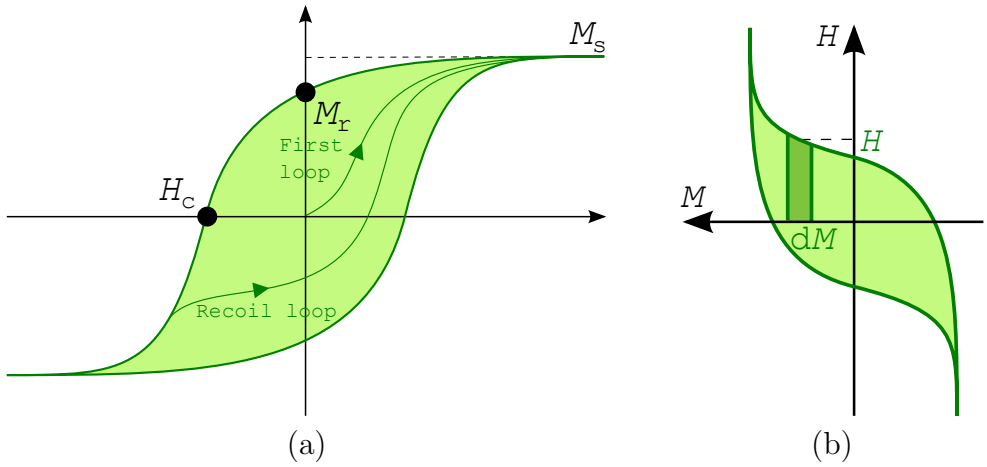

Figure I.3: (a) Typical hysteresis loop illustrating the definition of coercivity H_c, saturation M_s and remanent M_r magnetization. A minor (recoil) loop as well as a first magnetization loop are shown in thinner lines (b) The losses during a hysteresis loop equal the area of the loop.

Hysteresis loops are the most straightforward and widespread characterization of magnetic materials. We will thus discuss it in some details, thereby introducing important concepts for magnetic materials and their applications. We restrict the discussion to quasistatic hysteresis loops, *i.e.* nearly at local equilibrium. Dynamic and temperature effets require a specific discussion and microscopic modeling, which will be discussed in chapter sec.III, p.65.

Figure I.3 shows a typical hysteresis loop. We will speak of magnetization for the sake of simplicity. However the concepts discussed more generally apply to any other quantity involved in a hysteresis loop.

- **Symmetry** – Hysteresis loops are centro-symmetric, which reflect the time-reversal symmetry of Maxwell's equations ($H \to -H$ and $M \to -M$)

We will see in chapter V that hysteresis loops of certain heterostructured systems may be non-centro-symmetric, due to shifts along both the field and magnetization axes. This however does not contradict the principle of time-reversal symmetry, as such hysteresis loops are minor loops. Application of a sufficiently high field (let aside the practical availability of such a high field) would yield a centro-symmetric loop.

- **'Saturation' magnetization** – Due to Zeeman energy the magnetization tends to align along the applied field when the magnitude of the latter is large, associated with a saturation of the $M(H)$ curve. For this reason one often names saturation magnetization the resulting value of magnetization. We may normalize the loop with its value towards saturation, and get a function spanning in $[-1; 1]$.

Two remarks shall be made. First the 's' subscript brings some confusion between spontaneous magnetization, which is a microscopic quantity used in models such as magnetic ordering and that one may like to determine experimentally, and the experimental quantity estimated at saturation of the loop. The knowledge of the volume of the system (if a moment is measured) or a model (in case an experiment probes indirectly magnetization) is needed to link an experimental quantity with a magnetization. Intrinsic or extrinsic contributions to the absence of true saturation of hysteresis loops are also an issue.

- **Remanent magnetization** – starting from the application of an external magnetic field, we call remanent magnetization (namely, which remains) and write M_r or m_r when normalized, the value of magnetization remaining when the field is removed. After applying a positive (resp. negative) field, m_r is usually found in the range $[0; 1]$.

A negative remanence may occur in very special cases of heterostructured systems, as we will see in Chapter V.

- **Coercive field** – We call coercive field (namely, which opposes an action, here that of an applied magnetic field) and write H_c, the magnitude of field for which the loop crosses the x axis, *i.e.* when the average magnetization projected along the direction of the field vanishes.

- **Hysteresis and metastability** – We have mentioned that the sign of remanence depends on that of the magnetic field applied previously. This feature is named hysteresis: the $M(H)$ path followed for rising field is different from the descending path. Hysteresis results from the physical notion of metastability: for a given magnitude (and direction) of magnetic field, there may exist several equilibrium states of the system. These states are often only local minima of energy, and then said to be metastable. Coercivity and remanence are two signatures of hysteresis. The number of degrees of freedom increases with the size of a system, and so may do the number of metastable states in the energy landscape. The field history describes the sequence of magnetic fields (magnitude, sign and/or direction) applied before an observation. This history is crucial to determine in which stable or metastable state the system is left[I.5]. This highlight the important role played by spatially-revolved techniques (both microscopies and in reciprocal space) to deeply characterize the magnetic state of a system. Metastability implies features displayed during first-order transitions such as relaxation (over time) based on domain-wall movement, nucleation and the importance of extrinsic features in these such as defects. This implies that the modeling and engineering of the microstructure of materials is a key to control properties such as coercivity and remanence.

[I.5] The reverse is not true: it is not always possible to design a path in magnetic field liable to prepare the system in an arbitrary metastable state

- **Energy losses** – We often read the name magnetic energy, for a quantity including the Zeeman energy. This is improper from a thermodynamic point of view. The Zeeman quantity $-\mu_0\mathbf{M}.\mathbf{H}$ is the counterpart of $+PV$ for fluids thermodynamics: $\mathbf{H}$ is the vectorial intensive counterpart of pressure, and $\mathbf{M}$ is the vectorial extensive[I.6] counterpart of volume, *i.e.* a response of the system to the external stimulus. Thus, we should use the name density of magnetic enthalpy for the quantity $E_{\text{int}} - \mu_0\mathbf{M}.\mathbf{H}$, where E_{int} is the density of internal magnetic energy of the system[I.7], with analogy to $H = U + PV$. A readily-seen consequence is that the quantity $+\mu_0\mathbf{H}.\mathrm{d}\mathbf{M}$, analogous to $-P\mathrm{d}V$, is the density of work provided by the (external) operator and transferred to the system upon an infinitesimal magnetization process. Rotating the magnetization loop by 90° to consider M as x, we see that the area encompassed by the hysteresis loop measures the amount of work provided to the system upon the loop, often in the form of heat (Figure I.3b).

- **Functionalities of magnetic materials** – The quantities defined above allow us to consider various types of magnetic materials, and their use for applications. Metastability and remanence are key properties for memory applications such as hard disk drives (HDDs), as its sign keeps track of the previously applied field, defining so-called up and down states. Coercivity is crucial for permanent magnets, which must remain magnetized in a well-defined direction of the body with a large remanence, giving rise to forces and torques of crucial use in motors and actuators. In practice coercivities of one or two Teslas may be reached in the best permanent-magnet materials such as $SmCo_5$, Sm_2Co_{17} and $Nd_2Fe_{14}B$. The minimization of losses in the operation of permanent magnets and magnetic memories is important, both to minimize heating and for energy efficiency. Among applications requiring small losses are transformers and magnetic shielding. To achieve this one seeks both low coercivity and low remanence, which defines so-called soft magnetic materials. These materials are also of use in magnetic field sensors based on their magnetic susceptibility, providing linearity (low hysteresis) and sensitivity (large susceptibility $\mathrm{d}M/\mathrm{d}H$). A coercivity well below $10^{-3}\,\mathrm{A/m}$ (or 1.25 mT in terms of $\mu_0 H$) is obtained in the best soft magnetic materials, typically based on Permalloy ($Fe_{20}Ni_{80}$). On the reverse, some applications are based on losses such as induction stoves. There the magnitude of coercivity is a compromise between achieving large losses and the ability of the stove to produce large enough ac magnetic fields to reverse magnetization. Finally, in almost all applications the magnitude of magnetization determines the strength of the sought effect, such as force or energy of a permanent magnet, readability for sensors and memories, energy for transformers and induction heating.

- **Partial loops** – In order to gain more information about the magnetic material than with a simple hysteresis loop, one may measure a first magnetization loop (performed on a virgin or demagnetized sample) or a minor loop (also called partial loop or recoil loop), see Figure I.3a.

[I.6] or more precisely, the magnetic moment of the entire system $\int_V \mathbf{M}_{\text{s}}\mathrm{d}\mathbf{r}$.
[I.7] see part 3 for the description of contributions to E_{int}

We call intrinsic those properties of a material depending only on its composition and structure, and extrinsic those properties related to microscopic phenomena related to *e.g.* microstructure (crystallographic grains and grain boundaries), sample shape etc. For example, spontaneous magnetization is an intrinsic quantity, while remanence and coercivity are extrinsic quantities.

1.4 Domains and domain walls

Hysteresis loop, described in the previous section, concern a scalar and integrated quantity. It may thus hide details of magnetization (a vector quantity) at the microscopic level. Hysteresis loops must be seen as one out of many signature of magnetization reversal, not a full characterization. Various processes may determine the features of hysteresis loops described above. It is a major task of micromagnetism and magnetic microscopies to unravel these microscopic processes, with a view to improve or design new materials.

For instance remanence smaller than one may result from the rotation of magnetization or from the formation of magnetic domains etc. Magnetic domains are large regions where in each the magnetization is largely uniform, while this direction may vary from one domain to another. The existence of magnetic domains was postulated by Pierre Weiss in his mean field theory of magnetism in 1907, to explain why materials known to be magnetic may display no net moment at the macroscopic scale. The first direct proof of the existence of magnetic domains came only in 1931. This is due to the bitter technique, where nanoparticles are attracted by the loci of domain walls. In 1932 Bloch proposes an analytical description of the variation of magnetization between two domains. This area of transition is called a magnetic domain. The basis for the energetic study of magnetic domains was proposed in 1935 by Landau and Lifshitz.

Let us discuss what may drive the occurrence of magnetic domains, whereas domain walls imply a cost in exchange and other energies, see sec.5. There exists two reasons for this occurrence, which in practice often take place simultaneously. The first reason is energetics, where the cost of creating domain walls is balanced by the decrease the dipolar energy which would be that of a body remaining uniformly magnetized. This will be largely developed in chap.II. The second reason is magnetic history, which we have already mentioned when discussing hysteresis loops (see sec.1.3). For instance upon a partial demagnetization process up to the coercive field, domain walls may have been created, whose propagation will be frozen upon removal of the magnetic field.

2 Units in Magnetism

The use of various systems of units is a source of annoyance and errors in magnetism. A good reference about units is that by F. Cardarelli[8]. Conversion tables for magnetic units may also be found in many reference books in magnetism, such as those of S. Blundell[1] and J. M. D. Coey[3]. We shall here shortly consider three aspects:

- **The units** – A system of units consists in choosing a reference set of elemen-

tary physical quantities, allowing one to measure each physical quantity with a figure relative to the reference unit. All physical quantities may then be expressed as a combination of elementary quantities; the dimension of a quantity describes this combination. For a long time many different units were used, depending on location and their field of use. Besides the multiples were not the same in all systems. The wish to standardize physical units arose during the French revolution, and the Academy of Sciences was in charge of it. In 1791 the meter was the first unit defined, at the time as the ten millionth of the distance between the equator and a pole. Strictly speaking four types of dimensions are enough to describe all physical variables. A common choice is: length L, mass M, time T, and electrical current I. This lead to the emergence of the MKSA set of units, standing for **M**eter, **K**ilogram, **S**econd, **A**mpère for the four above-mentioned quantities. The Conférences Générale des Poids et Mesures (General Conference on Weighs and Measures), an international organization, decided of the creation of the Système International d'Unités (SI). In SI, other quantities have been progressively appended, which may in principle be defined based on MKSA, however whose independent naming is useful. The three extra SI units are thermodynamic temperature T (in Kelvin, K), luminous intensity (in candela, cd) and amount of matter (in mole, mol). The first two are linked with energy, while the latter is dimensionless. Finally, plane angle (in radian, rad) and solid angles (in steradian, sr) are called supplementary units. Another system than MKSA, of predominant use in the past, is the cgs system, standing for **C**entimeter, **G**ramm, and **S**econd. At first sight this system has no explicit units for electrical current or charge, which is a weakness with respect to MKSA, *e.g.* when it comes to check the dimension homogeneity of formulas. Several sub-systems were introduced to consider electric charges or magnetic moments, such as the esu (electrostatic units), emu (electromagnetic units), or the tentatively unifying Gauss system. In practice, when converting units between MKSA and cgs in magnetism one needs to consider the cgs-Gauss unit for electrical current, the Biot (Bi), equivalent to 10 A. Other names in use for the Biot are the abampere or the emu ampere. Based on the decomposition of any physical quantity in elementary dimensions, it is straightforward to convert quantities from one to another system. For magnetic induction B 1 T is the same as 10^4 G (Gauss), for magnetic moment μ 1 A.m^2 is equivalent to 10^3 emu and for magnetization M 1 A/m is equivalent to 10^{-3} emu/cm^3. In cgs-Gauss the unit for energy is erg, equivalent to 10^{-7} J. The issue of units would remain trivial, if restricted to converting numerical valus. The real pain is that different definitions exist to relate H, M and B, as detailed below.

- **Defining magnetic field H** – In SI induction is most often defined with $B = \mu_0(H+M)$, whereas in cgs-Gauss it is defined with $B = H+4\pi M$. The dimension of μ_0 comes out to be L.M.T^{-2}.I^{-2}, thus $\mu_0 = 4\pi\times10^{-7}$ m.kg.s^{-2}.A^{-2} in SI. Using the simple numerical conversion of units one finds: $\mu_0 = 4\pi$ cm.g.s^{-2}.Bi^{-2}. Similar to the absence of explicit unit for electrical current, it is often argued that μ_0 does not exist in cgs. The conversion of units reveals that one may consider it in the definition of M, with a numerical value 4π. However the definition de H differs, as the same quantity is written $\mu_0 H$ in SI, and $(\mu_0/4\pi)H$ in cgs-Gauss. Thus, the conversion of magnetic field H gives rise to an extra

4π coefficient, beyond powers of ten. This pitfall explain the need to use an extra unit, the Oersted, to express values for magnetic field H in cgs-Gauss. Then 1 Oe is equivalent to $(10^3/4\pi)\,\mathrm{A/m}$[I.8]. A painful consequence of the different definitions of H is that susceptibility $\chi = \mathrm{d}M/\mathrm{d}H$ differs by 4π between both systems, although is is a dimensionless quantity: $\chi_{\mathrm{cgs}} = (1/4\pi)\chi_{\mathrm{SI}}$. The same is true for demagnetizing coefficients defined by $H_{\mathrm{d}} = -NM$, with $N_{\mathrm{cgs}} = 4\pi N_{\mathrm{SI}}$.

- **Defining magnetization M** – we often find the writing $J = \mu_0 M$ in the literature. More problematic is the (rather rare) definition to use M_{s} instead of $\mu_0 M_{\mathrm{s}}$. It is for instance the case of the book of Stöhr and Siegmann[9], otherwise a very comprehensive book. These authors use the SI units, however define: $\mathbf{B} = \mu_0\mathbf{H} + \mathbf{M}$. This can be viewed as a compromise between cgs and SI, however has an impact on all formulas making use of M.

This section highlights that, beyond the mere conversion of numerical values, formulas depend on the definition used to link magnetization, magnetic field and induction. It is crucial to carefully check the system of units and definition used by authors before copy-pasting any formulas implying M, H or B.

3 The various types of magnetic energy

3.1 Introduction

There exists several sources of energy in magnetic systems, which we review in this section. For the sake of simplicity of vocabulary we restrict the following discussion to ferromagnetic materials, although all aspects may be extended to other types of orders. These energies will be described in the context of micromagnetism.

Micromagnetism is the name given to the investigation of the competition between these various energies, giving rise to characteristic magnetic length scales, and being the source of complexity of distributions of magnetization, which will be dealt with in chap.II.

Micromagnetism, be it numerical or analytical, is in most cases based on two assumptions: :

- The variation of the direction of magnetic moment from (atomic) site to site is sufficiently slow so that the discrete nature of matter may be ignored. Magnetization M and all other quantities are described in the approximation of continuous medium: they are continuous functions of the space variable $\mathbf{r}$.

- The norm M_{s} of the magnetization vector is constant and uniform in any homogeneous material. This norm may be that at zero or finite temperature. The latter case may be viewed as a mean-field approach.

Based on these two approximations for magnetization we often consider the function unitary vector function $\mathbf{m}(\mathbf{r})$ to describe magnetization distributions, such that $\mathbf{M}_{\mathrm{s}}(\mathbf{r}) = M_{\mathrm{s}}\mathbf{m}(\mathbf{r})$.

[I.8] In practice, the absence of μ_0 in the cgs system often results in the use of either Oersted or Gauss to evaluate magnetic field and induction.

3.2 Zeeman energy

The Zeeman energy pertains to the energy of magnetic moments in an external magnetic field. Its density is:

$$E_{\mathrm{Z}} = -\mu_0 \mathbf{M}.\mathbf{H} \tag{I.7}$$

E_{Z} tends to favor the alignement of magnetization along the applied field. As outlined above, this term should not be considered as a contribution to the internal energy of a system, however as giving rise to a magnetic enthalpy.

3.3 Magnetic anisotropy energy

The theory of magnetic ordering predicts the occurrence of spontaneous magnetization $\mathbf{M}_{\mathrm{s}}$, however with no restriction on its direction in space. In a real system the internal energy depends on the direction of $\mathbf{M}_{\mathrm{s}}$ with the underlying crystalline direction of the solid. This arises from the combined effect of crystal-field effects (coupling electron orbitals with the lattice) and spin-orbit effects (coupling orbital with spin moments).

This internal energy is called magnetocrystalline anisotropy energy, whose density will be written E_{mc} in these notes. The consequence of E_{mc} is the tendency for magnetization to align itself along certain axes (or in certain planes) of a solid, called easy directions. On the reverse, directions with a maximum of energy are called hard axes (or planes). Magnetic anisotropy is at the origin of coercivity, although the quantitative link between the two notions is complex, and will be introduced in chap.II.

The most general case may be described by a function $E_{\mathrm{mc}} = Kf(\theta, \varphi)$, where f is a dimensionless function. In principle any set of angular functions complying with the symmetry of the crystal lattice considered may be used as a basis to express f and thus E_{mc}. Whereas the orbital functions $Y_{l,m}$ of use in atomic physics may be suitable, in practice one uses simple trigonometric functions. Odd terms do not arise in magnetocrystalline anisotropy because of time-reversal symmetry. Group theory can be used to highlight the terms arising depending on the symmetry of the lattice.

For a cubic material one finds:

$$E_{\mathrm{mc,cub}} = K_{1\mathrm{c}} s + K_{2\mathrm{c}} p + K_{3\mathrm{c}} p^2 + \ldots \tag{I.8}$$

with $s = \alpha_1^2\alpha_2^2 + \alpha_2^2\alpha_3^2 + \alpha_3^2\alpha_1^2$ and $p = \alpha_1^2\alpha_2^2\alpha_3^2$. For hexagonal symmetry

$$E_{\mathrm{mc,hex}} = K_1 \sin^2\theta + K_2 \sin^4\theta + \ldots \tag{I.9}$$

where θ is the (polar) angle between $\mathbf{M}$ and the c axis. Here we dropped the azimuthal dependence because it is of sixth order, and that in practice the magnitude of anisotropy constants decreases sharply with its order. Thus for an hexagonal material the magnetocrystalline anisotropy is essentially uniaxial.

Group theory predicts the form of these formulas, however not the numerical values, which are material dependent. For example for Fe $K_{1\mathrm{c}} = 48\,\mathrm{kJ/m^3}$ so that the $< 001 >$ directions (resp. $< 111 >$) are easy (resp. hard) axes of magnetization, while for Ni $K_{1\mathrm{c}} = -5\,\mathrm{kJ/m^3}$ so that $< 001 >$ (resp. $< 111 >$) are hard (resp. easy)

axes of magnetization. In Co $K_1 = 410\,\mathrm{kJ/m^3}$ and the c axis of the hexagon is the sole easy axis of magnetization.

In many cases one often considers solely a second-order uniaxial energy:

$$E_{\mathrm{mc}} = K_{\mathrm{u}} \sin^2 \theta \tag{I.10}$$

It is indeed the leading term around the easy axis direction in all above-mentioned cases. We will see in sec.4 that it is also a form arising in the case of magnetostatic energy. It is therefore of particular relevance. Notice that it is the most simple trigonometric function compatible with time-reversal symmetry and giving rise to two energy minima, this liable to give rise to hysteresis. It is therefore sufficient for grasping the main physics yet with simple formulas in modeling.

Materials with low magnetic anisotropy energy are called soft magnetic materials, while materials with large magnetic anisotropy energy are called hard magnetic materials. The historical ground for these names dates back to the beginning of the twentieth century where steel was the main source of magnetic material. Mechanically softer materials were noticed to have a coercivity lower than that of mechanically harder materials.

One should also consider magnetoelastic anisotropy energy, written E_{mel}. E_{mel} is the magnetic energy associated with strain (deformation) of a material, either compressive, extensive or shear. E_{mel} may be viewed as the derivative of E_{mc} with respect to strain. In micromagnetism the anisotropy energy is described phenomenologically, ignoring all microscopic details. Thus we may consider the sum of E_{mc} and E_{mel}, written for instance E_{a} or E_K, a standing for anisotropy and K for an anisotropy constant.

3.4 Exchange energy

Exchange energy between neighboring sites may be written as:

$$\mathcal{E}_{12} = -J\mathbf{S}_1.\mathbf{S}_2 \tag{I.11}$$

J is positive for ferromagnetism, and tends to favor uniform magnetization. Let us outline the link with continous theory used in micromagnetism. We consider the textbook case of a (one-dimensional) chain of XY classical spins, *i.e.* whose direction of magnetization may be described by a single angle θ_i (Figure I.4). The hypothesis of slow variation of θ_i from site to site legitimates the expansion:

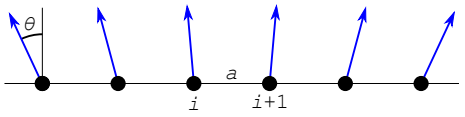

Figure I.4: Expansion of exchange with θ to link discrete exchange to continuous theory.

$$\begin{aligned} \mathcal{E}_{12} &= -JS^2 \cos(\delta\theta) \\ &= -JS^2 \left[1 - \frac{(\delta\theta)^2}{2}\right] \\ &= \mathrm{Cte} + \frac{JS^2a^2}{2}\left(\frac{\mathrm{d}\theta}{\mathrm{d}x}\right)^2 \end{aligned} \tag{I.12}$$

This equation may be generalized to a three dimensional system and moments allowed to point in any direction in space. Upon normalization with a^3 to express a density of energy, and forgetting about numerical factors related to the symmetry and number of nearest neighbors, one reaches:

$$E_{\text{ex}} = A\,(\boldsymbol{\nabla}\mathbf{m})^2\,. \tag{I.13}$$

We remind the reader that $\mathbf{m}(\mathbf{r})$ is the unit vector field describing the magnetization distribution. The writting $(\boldsymbol{\nabla}\mathbf{m})^2$ is a shortcut for $\sum_i \sum_j (\partial_{x_j} m_i)^2$, linked to Eq. (I.12). A is called the exchange, such as $A \approx (JS^2/2a)$. It is then clear that the unit for A is J/m, which we find also in Eq. (I.13). The order of magnitude of A for common magnetic materials such as Fe, Co and Ni is 10^{-11} J/m.

3.5 Magnetostatic energy

Magnetostatic energy, also called dipolar energy and written E_{d}, is the mutual Zeeman-type energy arising between all moments of a magnetic body through their stray field (itself called dipolar field and written H_{d}). When considering as a system an infinitesimal moment $\delta\mu\mathbf{M}_{\text{s}}\delta V$ the Zeeman energy provides the definition for enthalpy. However when considering the entire magnetic body as both the source of all magnetic field (dipolar field $\mathbf{H}_{\text{d}}$) and that of moments, this term contributes to the internal energy.

Dipolar energy is the most difficult contribution to handle in micromagnetism. Indeed, due to its non-local character is may be expressed analytically in only a very restricted number of simple situations. Its numerical evaluation is also very costly in computation time as all moments interact with all other moments; this contributes much to the practical limits of numerical simulation. Finally, due to the non-uniformity in direction and magnitude of the magnetic field created by a magnetic dipole, magnetostatic energy is a major source of the occurrence of non-uniform magnetization configurations in bulk as well as nanostructured materials, especially magnetic domains. For all these reasons we dwell a bit on this term in the following section.

3.6 Characteristic quantities

In the previous paragraphs we introduced the various sources of magnetic energy, and discussed the resulting tendencies on magnetization configurations one by one. When several energies are at play balances must be found and the physics is more complex. This is the realm of micromagnetism, the investigation of the arrangement of the magnetization vector field and magnetization dynamics. It is a major branch of nanomagnetism, and will be largely covered in chap.II.

It is a general situation in physics that when two or more effects compete, characteristic quantities emerge such as energy or length scales, and ratios. Here these will be built upon combination of M_{s} and H, a K constant such as K_{u} and A, which have different units. Characteristic length scales are of special importance in nanomagnetism, determining the size below which specific phenomena occur. Here we only make two preliminary remarks; more will discovered and discussed in the next chapter, ending with an overview.

Let us assume that in a problem only magnetic exchange and anisotropy compete. A and K_u are expressed respectively in J/m and J/m^3. The only way to combine these quantities to express a length scale, which we expect to arise in the problem, is $\Delta_u = \sqrt{A/K_u}$. We will call Δ_u the anisotropy exchange length[10] or Bloch parameter as often found in the literature. This is a direct measure of the width of a domain wall where magnetization rotates (limites by exchange) between two domains whose direction is set by K_u.

In a problem where exchange and dipolar energy compete, the two quantities at play are A and $K_d = (1/2)\mu_0 M_s^2$. In that case we may expect the occurrence of the length scale $\Delta_d = \sqrt{A/K_d} = \sqrt{2A/\mu_0 M_s^2}$, which we will call dipolar exchange length[6] or exchange length as more often found in the literature.

In usual magnetic materials Δ_u ranges from roughly one nanometer in the case of hard magnetic materials (high anisotropy), to several hundreds of nanometers in the case of soft magnetic materials (low anisotropy). Δ_d is of the order of 10 nm.

4 Handling dipolar interactions

4.1 Simple views on dipolar interactions

To grasp the general consequences of H_d let us first consider the interaction between two pinpoint magnetic dipoles $\boldsymbol{\mu}_1$ and $\boldsymbol{\mu}_2$, split by vector $\mathbf{r}$. Their mutual energy reads (see sec.I.5):

$$\mathcal{E}_d = -\frac{\mu_0}{4\pi r^3}\left[3\frac{(\boldsymbol{\mu}_1.\mathbf{r})(\boldsymbol{\mu}_2.\mathbf{r})}{r^2} - \boldsymbol{\mu}_1.\boldsymbol{\mu}_2\right] \tag{I.14}$$

We assume both moments to have a given direction $\mathbf{z}$, however with no constraint on their sign, either positive or negative. Let us determine their preferred respective orientation, either parallel or antiparallel depending on their locii, that of $\boldsymbol{\mu}_2$ being determined by vector r and the polar angle θ with respect to z (Figure I.5). Equation I.14 then reads:

$$E_{12} = \frac{\mu_0 \mu_1 \mu_2}{4\pi r^3}(1 - 3\cos^2\theta) \tag{I.15}$$

The ground state configuration being the one minimizing the energy, we see that parallel alignement is favored if $\cos^2\theta > 1/3$, that is within a cone of half-angle $\theta = 54.74°$, while antiparallel alignement is favored for intermediate angles (Figure I.5). Thus, under the effect of dipolar interactions two moments roughly placed along their easy axis tend to align parallel, while they tend to align antiparallel when placed next to each other. These rules rely on angles and not the length scale, and are thus identical at the macroscopic and microscopic scales. The example is that of permanent magnets, which are correctly approached by Ising spins.

The occurrence of a large part of space where antiparallel alignement is favored (outside the cone) makes us feel why bulk samples may be split in large blocks with different (*e.g.* antiparallel) directions of magnetization. These are magnetic domains. Beyond these handwavy arguments, the quantitative consideration of dipolar energy is outlined below in the framework of a continuous medium.

4.2 Ways to handle dipolar fields

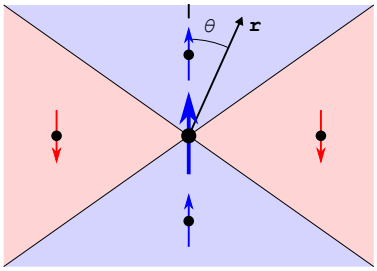

Figure I.5: Interaction between two Ising spins oriented along z. Parallel (resp. antiparallel) alignement is favored inside (resp. outside) a cone of half-angle 54.74°.

The total magnetostatic energy of a system with magnetization distribution $\mathbf{M}(\mathbf{r})$ reads :

$$\mathcal{E}_\mathrm{d} = -\frac{\mu_0}{2}\int \mathbf{M}(\mathbf{r}).\mathbf{H}_\mathrm{d}(\mathbf{r})\,\mathrm{d}^3r. \tag{I.16}$$

The pre-factor $\frac{1}{2}$ results from the need not to count twice the mutual energy of each set of two elementary dipoles taken together. The decomposition of a macroscopic body in elementary magnetic moments and performing a three-dimensional integral is not a practical solution to evaluate $\mathcal{E}_\mathrm{d}$. It is often better to proceed similarly to electrostatics, with $\mathrm{div}\,\mathbf{E} = \rho/\epsilon_0$ being replaced by $\mathrm{div}\,\mathbf{H}_\mathrm{d} = -\mathrm{div}\,\mathbf{M}$ (derived from the definition of $\mathbf{B}$, and Maxwell's equation $\mathrm{div}\,\mathbf{B} = \mathbf{0}$). Within this analogy, $\rho = -\mathrm{div}\,\mathbf{M}$ are called magnetic volume charges. A little algebra shows that the singularity of $\mathrm{div}\,\mathbf{M}$ that may arise at the border of magnetized bodies (M_s going abruptly from a finite value to zero on either side of the surface of the body) can be lifted by introducing the concept of surface charges $\sigma = \mathbf{M}.\mathbf{n}$. One has finally:

$$\mathbf{H}_\mathrm{d}(\mathbf{r}) = \int \frac{\rho(\mathbf{r}')\,(\mathbf{r}-\mathbf{r}')}{4\pi|\mathbf{r}-\mathbf{r}'|^3}\mathrm{d}^3r' + \oint \frac{\sigma(\mathbf{r}')\,(\mathbf{r}-\mathbf{r}')}{4\pi|\mathbf{r}-\mathbf{r}'|^3}.\mathrm{d}\mathbf{S} \tag{I.17}$$

$\mathrm{d}\mathbf{S}$ with $\mathbf{S}$ oriented towards the outside of the body is the elementary integration surface. This set, notice that $\mathbf{H}_\mathrm{d}$ has a zero rotational and thus derives from a potential: $\mathbf{H}_\mathrm{d} = -\mathbf{grad}\,\phi_\mathrm{d}$. Equation I.16 may then worked out, integrating in parts:

$$\begin{aligned}
\mathcal{E}_\mathrm{d} &= \frac{1}{2}\mu_0 \int \mathbf{M}(\mathbf{r}).\mathbf{grad}\,\phi_\mathrm{d}(\mathbf{r})\,\mathrm{d}^3r && \text{(I.18)}\\
&= \frac{1}{2}\mu_0 \int M_i(\mathbf{r}).\partial_{x_i}\phi_\mathrm{d}\,\mathrm{d}^3r && \text{(I.19)}\\
&= \left[\frac{1}{2}\mu_0\phi_\mathrm{d}M_i\right]^\infty - \frac{1}{2}\mu_0\int(\partial_{x_i}M_i)\phi_\mathrm{d}\,\mathrm{d}^3r && \text{(I.20)}\\
& && \text{(I.21)}
\end{aligned}$$

The first term cancels for a finite size system, and one finds a very practical formulation:

$$\mathcal{E}_\mathrm{d} = \frac{1}{2}\mu_0\left(\int \rho\phi_\mathrm{d}\,\mathrm{d}^3r + \int \sigma\phi_\mathrm{d}\,\mathrm{d}S\right). \tag{I.22}$$

Another equivalent formulation may be demonstrated:

$$\mathcal{E}_\mathrm{d} = \frac{1}{2}\mu_0\int H_\mathrm{d}^2\,\mathrm{d}^3r \tag{I.23}$$

where integration if performed other the entire space. From the latter we infer that E_d is always positive or zero. Equation I.22 shows that if dipolar energy alone si considered, its effect is to promote configurations of magnetization free of volume and surface magnetic charges. Such configurations are thus ground states (possibly degenerate) in the case where dipolar energy alone is involved.

- The tendency to cancel surface magnetic charges implies a very general rule for soft magnetic materials: their magnetization tends to remain parallel to the edges and surfaces of the system.
- The name dipolar field is a synonym for magnetostatic field. It refers to all magnetic fields created by a distribution of magnetization or magnetic moments in space. The name stray field refers to that part of dipolar field, occurring outside the body responsible for this field. The name demagnetizing field refers to that part of dipolar field, occurring inside the body source of this field; the explanation for this name will be given later on.

The term dipolar brings some confusion between two notions. The first notion is dipolar (field or energy) in the general sense of magnetostatic. The name dipolar stems from the fact that to compute total magnetostatic quantities of a magnetic body, whatever its complexity, one way is to decompose it into elementary magnetic dipoles and perform an integration; the resulting calculated quantities are then exact. The second notion is magnetic fields or energies arising from idealized pinpoint magnetic dipoles, and obeying Eq. (I.14). When using the name dipolar to refer to the interactions between two bodies, one may think either that we compute the exact magnetostatic energy based on the integration of elementary dipoles, or that we replace the two finite-size bodies with pinpoint dipoles for the sake of simplicity, yielding on the reverse an approach evaluation. In that latter case one may add extra terms, called multipolar, to improve the accuracy of the approximation. **To avoid confusion one should stress explicitly the approximation in the latter case, for instance mentioning the use of a point dipole approximation**.

4.3 Demagnetizing factors

Demagnetizing factors (or coefficients) are a simple concept providing figures for the magnetostatic energy of a body. Eq. (I.17) applied to uniform magnetization retains only the surface contribution

$$\mathbf{H}_\mathrm{d}(\mathbf{r}) = M_\mathrm{s} \int \frac{(\mathbf{r}-\mathbf{r}')}{4\pi|\mathbf{r}-\mathbf{r}'|^3}\, m_i n_i \,\mathrm{d}S(\mathbf{r}') \tag{I.24}$$

with $\mathbf{M} \equiv M_\mathrm{s}\mathbf{m}$, $\mathbf{m} = m_i\mathbf{u}_i$ and $\mathbf{n} = n_i\mathbf{u}_i$, with Einstein's summation notation. $\mathbf{n}$ is the local normal to the surface, oriented towards the outside of the body. Injecting this equation into Eq. (I.16) yields after straightforward algebra a compact formula for the density of demagnetizing energy:

$$E_\mathrm{d} = K_\mathrm{d}\ {}^\mathrm{t}\mathbf{m}.\overline{\overline{\mathbf{N}}}.\mathbf{m} \tag{I.25}$$

with $K_\mathrm{d} = \frac{1}{2}\mu_0 M_\mathrm{s}^2$, and $\overline{\overline{\mathbf{N}}}$ a 3×3 matrix with coefficients:

Table I.3: Demagnetizing factors for cases of practical use

Case	Demagnetizing factor	Note
Slab	$N_x = -1$	Normal along x
General ellipsoid	$N_x = \frac{1}{2}abc \int_0^\infty \left[(a^2+\eta)\sqrt{(a^2+\eta)(b^2+\eta)(c^2+\eta)}\right]^{-1} \mathrm{d}\eta$	
Prolate revolution ellipsoid	$N_x = \frac{\alpha^2}{1-\alpha^2}\left[\frac{1}{\sqrt{1-\alpha^2}} \operatorname{arg\,sinh}\left(\frac{\sqrt{1-\alpha^2}}{\alpha}\right) - 1\right]$	$\alpha = c/a < 1$
Oblate revolution ellipsoid	$N_x = \frac{\alpha^2}{\alpha^2-1}\left[1 - \frac{1}{\sqrt{\alpha^2-1}} \arcsin\left(\frac{\sqrt{\alpha^2-1}}{\alpha}\right)\right]$	$\alpha = c/a > 1$
Cylinder with elliptical section	$N_x = 0$, $N_y = c/(b+c)$ and $N_z = b/(b+c)$	Axis along x
Prism	Analytical however long formula	See: [6] or [13]

$$N_{ij} = \int \mathrm{d}^3 r \int \frac{n_i(\mathbf{u})\,(\mathbf{r}-\mathbf{r}')_j}{4\pi|\mathbf{r}-\mathbf{u}|^3}\,\mathrm{d}S(\mathbf{u}) \tag{I.26}$$

$\overline{\overline{\mathbf{N}}}$ is called the demagnetizing matrix. It may be shown that $\overline{\overline{\mathbf{N}}}$ is symmetric and positive, and thus can be diagonalized. The set of xyz axes upon diagonalization are called the main or major axes. The coefficients N'_{ii} of the diagonal matrix are called the demagnetizing coefficients and will be written N_i hereafter as a shortcut. Along these axes it is readily seen that the following is true for the average demagnetizing field, providing a simple interpretation of demagnetizing factors:

$$\langle \mathbf{H}_{\mathrm{d},i} \rangle = -N_i \mathbf{M}. \tag{I.27}$$

$\overline{\overline{\mathbf{N}}}$ yield a quadratic form, so that only second-order anisotropies can arise from dipolar energy, at least for perfectly uniform samples[I.9].

It can be shown that $\mathrm{Tr}(\mathbf{N}) = 1$, so that $N_x + N_y + N_z = 1$. Analytical formulas for N_i's may be found for revolution ellipsoids[11], prisms[12, 13] (Figure I.6), cylinders of finite length[14, 15, 16], and tetrahedrons[17, 18]. Some formulas are gathered in Table I.3. For other geometries micromagnetic codes or Fourier-space computations[18] may be used.

While all the above is true for bodies with an arbitrary shape, not even necessarily connected, a special subset of bodies is worth considering: that of shapes embodied by a polynomial surface of degree at most two. To these belong slabs, ellipsoids and cylinders with an ellipsoidal cross-section. In that very special case it may be shown within the non-trivial theory of integration in space[19] that Eq. (I.27) is then true locally: in the case of uniform magnetization, H_d is uniform and equal to $-N_i\mathbf{M}$ when $\mathbf{M}$ is aligned parallel to one of the major directions. This allows the torque on magnetization to be zero, and thus ensures the self-consistency of the assumption of uniform magnetization. This makes the application of demagnetizing factors of somewhat higher reliability than for bodies with an arbitrary shape. Notice, however, that self-consistency does not necessarily imply that the uniform state is stable and a ground state.

[I.9] see sec.4.4 for effects due to non-uniformities

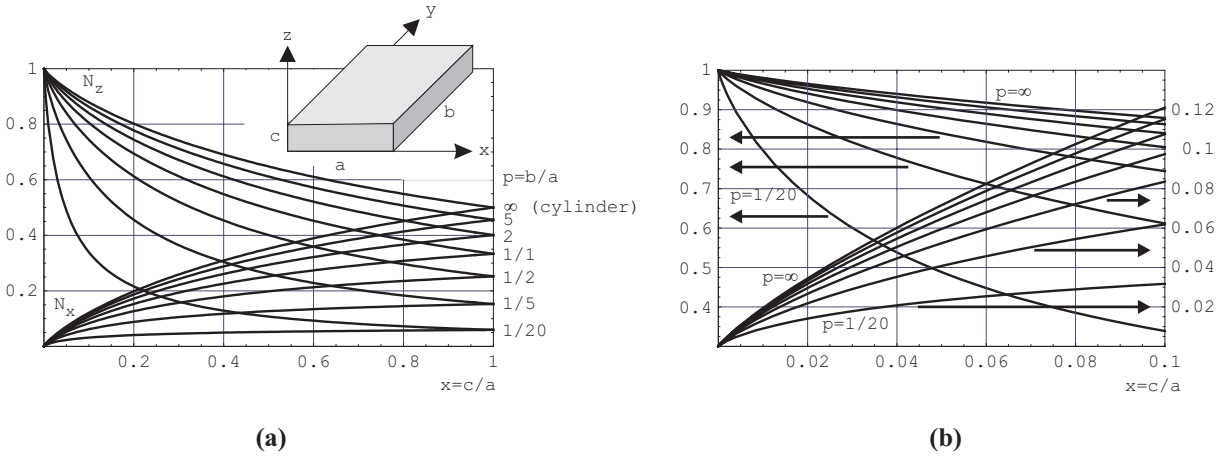

Figure I.6: Numerical evaluation of demagnetizing factors for prisms. (a) is the full plot, while (b) is en enlargement for flat prisms.

Demagnetizing factors are derived based on the assumption of uniform magnetization. While this assumption allows demagnetizing factors to be defined and calculated analytically or numerically, care should be taken when applying these to practical cases, where magnetization configurations may not be uniform.

5 The Bloch domain wall

The existence of magnetic domains was suggested by Pierre WEISS in his mean field theory of Magnetism in 1907. Magnetic domains were postulated to explain why large bodies made of a ferromagnetic materials could display no net magnetic moment under zero external magnetic field. Their existence was confirmed only in 1931 with a bitter technique, based on magnetic nanoparticles decorating the locii of domain walls because these particles are attracted by the local gradient of magnetic field. This example highlights the importance of magnetic microscopy in the progress of micromagnetism. In 1932 Bloch provides an analytical solution in a simple case to describe the region of transition between two magnetic domains, which is named a magnetic domain wall. At this stage we do not discuss the origin of magnetic domains, however focus on the model of a domain wall.

The Bloch model is one-dimensional, *i.e.* considers a chain of spins. The idea is to describe the transition between two three-dimensional domains (volumes) in the form of a two-dimensional object with translational invariance in the plane of the domain wall. It is assumed that magnetization remains in the plane of the domain wall, a configuration associated with zero volume charges $-\mathrm{div}\,\mathbf{M}$ and thus associated zero dipolar energy. The only energies at play are then the exchange energy, and the magnetic anisotropy energy which is assumed to be uniaxial and of second order. Under these assumptions the density of magnetic energy reads:

$$E(x) = K_\mathrm{u} \sin^2\theta + A\,(\partial_x \theta)^2 \tag{I.28}$$

where x if the position along the chain of spins. The case thus consists in exhibiting the magnetic configuration which minimizes the total energy

$$\mathcal{E} = \int_{-\infty}^{+\infty} [E_K(x) + E_\mathrm{ech}(x)]\mathrm{d}x. \tag{I.29}$$

while fulfilling boundary conditions compatible for a 180° domain wall: $\theta(-\infty) = 0$ and $\theta(+\infty) = \pi$.

5.1 Simple variational model

This paragraph proposes an approached solution for a domain wall, however appealing for its simplicity and ability to highlight the physics at play, and a reasonable numerical result. We consider the following model for a domain wall of width ℓ: $\theta = 0$ for $x < -\ell/2$, $\theta = \pi(x + \ell/2)$ for $x \in [-\ell/2; \ell/2]$ and $\theta = \pi$ for $x > \ell/2$. In a variational approach we search for the value ℓ_var which minimizes Eq. (I.29), after integration: $\mathcal{E} = K_\mathrm{u}\ell/2 + A\pi^2/\ell$. The minimization yields $\ell_\mathrm{var} = \pi\sqrt{2}\sqrt{A/K_\mathrm{u}}$ and $\mathcal{E}_\mathrm{var} = \pi\sqrt{2}\sqrt{AK_\mathrm{u}}$ is the associated energy.

Letting aside the factor $\pi\sqrt{2}$ a simple variational model highlights the relevance of the Bloch parameter Δ_u defined previously. How may we read this formula? Exchange only would tend to enlarge the domain wall, hence its occurrence at the numerator. To the reverse, the anisotropy energy gives rise to a cost of energy in the core of the domain wall. This tends to decrease its width, explaining its occurrence at the denominator.

5.2 Exact model

The exact profile of a Bloch domain wall may be derived using the principle of functional minimization to find the function θ minimizing $\mathcal{E}$. It may be shown that the principle of minimization is equivalent to the so-called Euler equation:

$$\frac{\partial E}{\partial \theta} = \frac{\mathrm{d}}{\mathrm{d}x}\left[\frac{\partial E}{\partial(\frac{\mathrm{d}\theta}{\mathrm{d}x})}\right] \tag{I.30}$$

Using a condensed notation this reads:

$$\partial_\theta E = \mathrm{d}_x\left(\partial_{(\mathrm{d}_x\theta)} E\right) \tag{I.31}$$

Considering a magnetic system described by Eq. (I.29) one finds:

$$\begin{aligned} \mathrm{d}_\theta E_K &= \mathrm{d}_x\left(2A\partial_x\theta\right) && \text{(I.32)}\\ &= 2A\partial_{xx}\theta && \text{(I.33)} \end{aligned}$$

Upon multiplying both parts by $\partial_x\theta$ and integration, this reads:

$$\begin{aligned} E_K(x) - E_K(a) &= A\left[\partial_x\theta(x)\right]^2 - A\left[\partial_x\theta(a)\right]^2 \\ &= E_{\mathrm{ex}}(x) - E_{\mathrm{ex}}(a) && \text{(I.34)} \end{aligned}$$

a is the origin of integration, here chosen as the center of the domain wall. Considering two semi-infinite domains with equal local density of energy, E is stationary (minimum) in both domains, and by convention may be chosen zero with no loss of generality. Equation I.34 applied to $\pm\infty$ shows that $E_K(a) = E_{\mathrm{ex}}(a)$, and finally:

$$\forall x \quad E_K(x) = E_{\mathrm{ex}}(x) \tag{I.35}$$

We hereby reach a general and very important feature of a domain wall separating two semi-infinite domains under zero applied field: the local density of anisotropy and exchange energy are equally parted **at any location of the system**. The equal parting of energy considerably eases the integration to get the areal density of the domain wall[I.10]:

[I.10] We set arbitrarily $\partial_x\theta > 0$ without loss of generality, using the symmetry $x \to -x$.

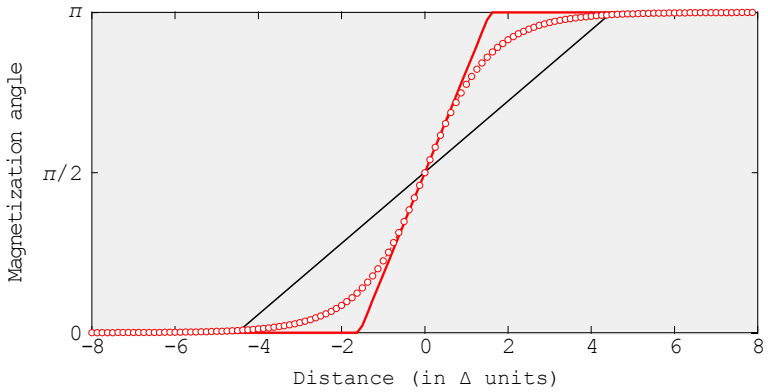

Figure I.7: Exact solution for the profile of the Bloch domain wall (red dots), along with its asymptote (red line). The lowest-energy solution of the linear variational model is displayed as a black line.

$$\begin{aligned}
\mathcal{E} &= 2\int_{-\infty}^{+\infty} A\,(\mathrm{d}_x\theta)^2\ \mathrm{d}x \\
&= 2\int_{-\infty}^{+\infty} E_K(x)\,\mathrm{d}x \\
&= 2\int_{-\infty}^{+\infty} \sqrt{AE_K(x)}\mathrm{d}_x\theta\,\mathrm{d}x \\
&= 2\int_{\theta(-\infty)}^{\theta(+\infty)} \sqrt{AE_K(\theta)}\,\mathrm{d}\theta
\end{aligned} \tag{I.36}$$

The energy of the domain wall may thus be expressed from the anisotropy of energy alone, without requiring solving the profile of the domain wall, which may be interesting to avoid calculations or when the latter cannot be solved.

Let us come back to the textbook case of the functional I.28. After some algebra one finds for the exact solution:

$$\theta_{\mathrm{ex}}(x) = 2\arctan\left[\exp(x/\Delta_{\mathrm{u}})\right] \tag{I.37}$$

$$\mathcal{E}_{\mathrm{ex}} = 4\sqrt{AK_{\mathrm{u}}}. \tag{I.38}$$

$\Delta_{\mathrm{u}} = \sqrt{A/K_{\mathrm{u}}}$ is of course confirmed to be a natural measure for the width of a domain wall. The exact solution along with that of the variational model are displayed on Figure I.7. Despite its crudeness, the latter is rather good, for both the wall profile and its energy: the true factor afore $\sqrt{AK_{\mathrm{u}}}$ equals 4 against $\pi\sqrt{2} \approx 4.44$ in the variational model. It is trivial to notice that $\mathcal{E}_{\mathrm{var}} > \mathcal{E}_{\mathrm{ex}}$, as the energy of a test function may only be larger than the energy of the minimum functional. It shall be noticed that the equal parting of energy is retained in the variational model, however only in its global form, not locally.

5.3 Defining the width of a domain wall

Several definitions for the width δ_{W} of a domain wall have been proposed (see *e.g.* Ref.[6], p.219).

The most common definition was introduced by Lilley[20]. It is based on the intercept of the asymptotes (the domain) with the tangent at the origin (the wall) of the curve $\theta(x)$. This yields $\delta_{\mathrm{L}} = \pi\sqrt{A/K_{\mathrm{u}}} = \pi\Delta_{\mathrm{u}}$ for the exact solution, and $\delta_{\mathrm{L}} = \ell_{\mathrm{variationel}} = \sqrt{2}\Delta_{\mathrm{u}}$ for the linear variational model.

Some call Δ_{u} the domain wall width. To avoid any confusion is it advised to keep the name Bloch parameter for this quantity.

A second definition consists in using the asymptotes of the curve $\cos\theta(x)$, instead of that of $\theta(x)$. On then finds $\delta_{\mathrm{m}} = 2\sqrt{A/K_{\mathrm{u}}}$, both in the exact and variational models.

A third definition is $\delta_{\mathrm{F}} = \int_{-\infty}^{+\infty} \sin\theta(x)\mathrm{d}x$. In the present case of a uniaxial anisotropy of second order one finds $\delta_{\mathrm{F}} = \delta_{\mathrm{L}}$.

The latter two definitions are more suited for the analysis of domain walls investigated by magnetic microscopies probing the projection of magnetization in a given direction. Besides, δ_{F} is based on an integration. It can thus be applied to any type of domain wall, whereas the definitions of Lilley and δ_{m} may be ambiguous in materials with high anisotropy constants, with domain wall profiles potentially displaying several inflexion points.

The use of cos and sin fonctions in the definitions δ_{m} and δ_{F} is dependent on the starting and ending angles of the domain wall, here 0 and π. For other choices or domain walls with angle differing from 180°, these definitions shall be modified.

6 Magnetometry and magnetic imaging

There exists many techniques to probe magnetic materials. Due to the small amounts to be probed, and the need to understand magnetization configurations, high sensitivity and/or microscopies are of particular interest for nanomagnetism. There exists no such thing as a universal characterization technique, that would be superior to all others. Each of them has its advantages and disadvantages in terms of versatility, space and time resolution, chemical sensitivity etc. The combination of several such techniques is often beneficial to gain the full understanding of a system.

Here a quick and non-exhaustive look is proposed over some techniques that have proven useful in nanomagnetism. In-depth reviews may be found elsewhere[6, 21, 22, 23].

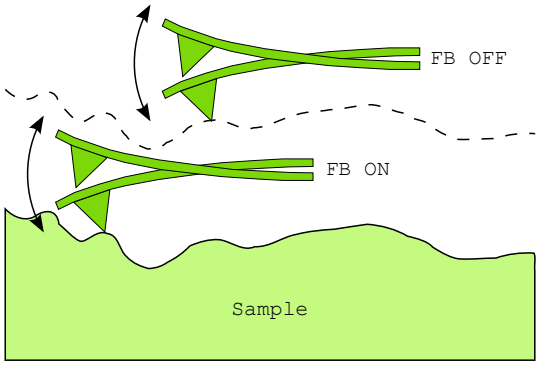

Figure I.8: Principle of the two-pass procedure usually implemented for MFM imaging.

6.1 Extraction magnetometers

6.2 Faraday and Kerr effects

6.3 X-ray Magnetic Dichroism techniques

6.3.A X-RAY MAGNETIC CIRCULAR DICHROISM

6.3.B XMCD PHOTO-EMISSION ELECTRON MICROSCOPY

6.3.C XMCD TRANSMISSION X-RAY MICROSCOPY

6.4 Near-field microscopies

6.4.A MAGNETIC FORCE MICROSCOPY

Magnetic Force Microscopy (MFM) is derived from Atomic Force Microscopy, for which good reviews are available. Along with Kerr microscopy, it is the most popular magnetic microscopy technique owing to its combination of moderate cost, reasonable spatial resolution (routinely 25-50 nm) and versatility. Good reviews are available for both AFM[24] and MFM[22, 21].

AFM and MFM probe forces between a sample and a sharp tip. The tip is non-magnetic in the former case, and coated with a few tens of nanometers of magnetic material in the latter case. The forces are estimated through the displacement of a soft cantilever holding the tip, usually monitoring the deflection of a laser reflected at the backside of the cantilever. The most common working scheme of MFM is an ac technique: while the cantilever is mechanically excited close to its resonance frequency f_0 (or more conveniently written as the angular velocity $\omega_0 = 2\pi f_0$), the phase undergoes a shift proportional to the vertical gradient of the (vertical) force $\partial F/\partial z$ felt by the tip: $\Delta\varphi = -(Q/k)\partial_z F$. In practice magnetic images are gathered using a so-called two-pass technique: each line of a scan is first conducted in the tapping mode with strong hard-sphere repulsive forces probing mostly topography (so-called first pass), then a second pass is conducted flying at constant height (called the lift height) above the sample based on the information gathered during the first pass. Forces such as Van der Waals are assumed to be constant during the second pass, and the forces measured are then ascribed to long-range forces such as magnetic.

The difficult point with MFM is the interpretation of the images, and the possible mutual interaction between tip and sample. A basic discussion of MFM is proposed in the Problems section, p.37. A summary of the expected signal measured is provided in Table I.4.

Table I.4: Expected MFM signal with respect to the vertical component $H_{\mathrm{d},z}$ of the stray field in static (cantilever deflection) and dynamic (frequency shift during the second pass) modes versus the model for the MFM tip.

Tip model	Static response	Dynamic response
Monopole	$H_{\mathrm{d},z}$	$\partial H_{\mathrm{d},z}/\partial z$
Dipole	$\partial H_{\mathrm{d},z}/\partial z$	$\partial^2 H_{\mathrm{d},z}/\partial z^2$

6.4.b Spin-polarized Scanning Tunneling Microscopy

6.5 Electron microscopies

6.5.a Lorentz microscopy

6.5.b Scanning Electron Microscopy with Polarization Analysis (SEMPA)

6.5.c Spin-Polarized Low-Energy Electron Microscopy (SPLEEM)

Problems for Chapter I

Problem 1: More about units

Here we derive the dimensions for physical quantities of use in magnetism, and their conversions between cgs-Gauss and SI.

1.1. Notations

We use the following notations:

- X is a physical quantity, such as force in $F = mg$. It may be written $\mathbf{X}$ for vectors.
- $[X]$ is the dimension of X. As a shortcut we will use a vector to summarize the powers of the fundamental units length (L), mass (M), time (T) and electrical current (I). For example, speed and electrical charges read: $[v] = [L] - [T] = [1\ 0\ {-1}\ 0]$ and $[q] = [I] + [T] = [0\ 0\ 1\ 1]$. We use shortcuts $[L]$, $[M]$, $[T]$ and $[I]$ for the four fundamental dimensions.
- In a system of units α (*e.g.* SI or cgs-Gauss) a physical quantity is evaluated numerically based on the unit physical quantities: $X = X_\alpha \langle X \rangle_\alpha$. X_α is a number, while $\langle X \rangle_\alpha$ is the standard (*i.e.*, used as unity) for the physical quantity in the system considered. For example $\langle L \rangle_{\rm SI}$ is a length of one meter, while $\langle L \rangle_{\rm cgs}$ is a length of one centimeter: $\langle L \rangle_{\rm SI} = 100 \langle L \rangle_{\rm cgs}$. For derived dimensions we use the matrix notation. For example the unit quantity for speed in system α would be written $[1\ 0\ -1\ 0]_\alpha$.

1.2. Expressing dimensions

- Based on laws for mechanics, find dimensions for force F, energy $\mathcal{E}$ and power $\mathcal{P}$, and their volume density E and P.
- Based on the above, find dimensions for electric field $\mathbf{E}$, voltage U, resistance R, resistivity ρ, permittivity ϵ_0.
- Find dimensions for magnetic field and magnetization $\mathbf{H}$ and $\mathbf{M}$, induction $\mathbf{B}$ and permeability μ_0.

1.3. Conversions

Physics does not depend on the choice for a system of units, so doesn't any physical quantity X. The conversions between its numerical values X_α and X_β in two such systems is readily obtained from the relationship between $\langle X\rangle_\alpha$ and $\langle X\rangle_\beta$, writing: $X = X_\alpha\langle X\rangle_\alpha = X_\beta\langle X\rangle_\beta$. Let us consider length l as a example. $l = l_{\rm SI}\langle L\rangle_{\rm SI} = l_{\rm cgs}\langle L\rangle_{\rm cgs}$. As $\langle L\rangle_{\rm SI} = 100\langle L\rangle_{\rm cgs}$ we readily have: $l_{\rm SI} = (1/100)l_{\rm cgs}$. Thus the numerical value for the length of an olympic swimming pool is 5000 in cgs, and 50 in SI. For derived units (combination of elementary units), $\langle X\rangle_\alpha$ is decomposed in elementary units in both systems, whose relationship is known. For example for speed: $\langle v\rangle_\alpha = \langle L\rangle_\alpha\langle T\rangle_\alpha^{-1}$. Notice that in the cgs-Gauss system, the unit for electric charge current may be considered as existing and named Biot or abampère, equivalent to 10 A.

Exhibit the conversion factor for these various quantities, of use for magnetism:

- Energy $\mathcal{E}$, energy per unit area $E_{\rm s}$, energy per unit volume E. The unit for energy in the cgs-Gauss system is called erg.
- Express the conversion for magnetic induction B and magnetization M, whose units in cgs-Gauss are called Gauss and emu, respectively. Express related quantities such as magnetic flux ϕ and magnetic moment μ.
- Let us recall that magnetic field is defined in SI with $B = \mu_0(H+M)$, whereas in cgs-Gauss with $B = H + 4\pi M$, with the unit called Oersted. Express the conversion for μ_0 and comment. Then express the conversion for magnetic field H.
- Discuss the cases of magnetic susceptibility $\chi = {\rm d}M/{\rm d}H$ and demagnetizing coefficients defined by $H_{\rm d} = -NM$.

Problem 2: More about the Bloch domain wall

The purpose of this problem is to go deeper in the mathematics describing the textbook case of the Bloch domain wall discussed in sec.5. We recall the following shortcuts: $\partial_x\theta$ for $\partial\theta/\partial x$ and $\partial_x^n\theta$ for $\partial^n\theta/\partial x^n$.

2.1. Euler-Lagrange equation

We will seek to exhibit a magnetization configuration that minimizes an energy density integrated over an entire system: $\mathcal{E} = \int E(\mathbf{r}){\rm d}\mathbf{r}$. Finding the minimum of a continuous quantity integrated over space is a common problem solved through Euler-Lagrange equation, which we will deal with in a textbook one-dimensional framework here.

Let us consider a microscopic variable defined as $F(\theta, {\rm d}_x\theta)$, where x is the spatial coordinate and θ a quantity defined at each point. In the case of micromagnetism we will have:

$$F\left(\theta, {\rm d}_x\theta\right) = A\left({\rm d}_x\theta\right)^2 + E(\theta) \tag{I.39}$$

When applied to micromagnetism $E(\theta)$ may contain anisotropy, dipolar and Zeeman terms. We define the integrated quantity:

$$\mathcal{F} = \int_A^B F\left(\theta, \mathrm{d}_x\theta\right) \mathrm{d}x + E_A(\theta) + E_B(\theta). \tag{I.40}$$

A and B are the boundaries of the system, while $E_A(\theta)$ and $E_B(\theta)$ are surface energy terms.

Let us consider an infinitesimal function variation $\delta\theta(x)$ of θ. Show that extrema of $\mathcal{F}$ are determined by the following relationships:

$$\begin{aligned} \partial_\theta F - \mathrm{d}_x\left(\partial_{\mathrm{d}_x\theta} F\right) &= 0 && \text{(I.41)} \\ \mathrm{d}_\theta E_A - \partial_{\mathrm{d}_x\theta} F|_A &= 0 && \text{(I.42)} \\ \mathrm{d}_\theta E_B + \partial_{\mathrm{d}_x\theta} F|_B &= 0 && \text{(I.43)} \end{aligned}$$

Notice that equations Eq. (I.42) and Eq. (I.43) differ in sign because a surface quantity should be defined with respect to the unit vector normal to the surface, with a unique convention for the sense, such as the outwards normal. Here the abscissa x is outwards for point$B$ however inwards at A. An alternative microscopic explanation would be that for a given sign of $\mathrm{d}_x\theta$ the exchange torque exerted on a moment to the right (at point B) is opposite to that exerted to the left (at point A), whereas the torque exerted by a surface anisotropy energy solely depends on θ.

2.2. Micromagnetic Euler equation

Apply the above equations to the case of micromagnetism [Eq. (I.39)]. Starting from Eq. (I.41) exhibit a differential equation linking $E[\theta(x)]$ with $\mathrm{d}_x\theta$. Equations I.42-I.43 are called Brown equations. $E_A(\theta)$ and $E_B(\theta)$ may be surface magnetic anisotropy, for instance. Discuss the microscopic meaning of these equations.

Comment the special case of free boundary conditions (all bulk and surface energy terms vanish at A and B), in terms of energy partition. Now on we switch back to the physics notation $\mathcal{E}$ for the total energy, instead of $\mathcal{F}$. Show that it can be expressed as:

$$\mathcal{E} = 2\int_{\theta(A)}^{\theta(B)} \sqrt{AE(\theta)}\, \mathrm{d}\theta \tag{I.44}$$

2.3. The Bloch domain wall

Let us assume the following free boundary conditions, mimicking two extended domains with opposite magnetization vectors separated by a domain wall whose profile we propose to derive here: $\theta(-\infty) = 0$ and $\theta(+\infty) = \pi$. We will assume the simplest form of magnetic anisotropy, uniaxial of second order: $E(\theta) = K_\mathrm{u} \sin^2\theta$.

Based on a dimensional analysis give approximate expressions for both the domain wall width δ and the domain wall energy $\mathcal{E}$. What are the SI units for $\mathcal{E}$? Discuss the form of these quantities in relation with the meaning and effects of exchange and anisotropy.

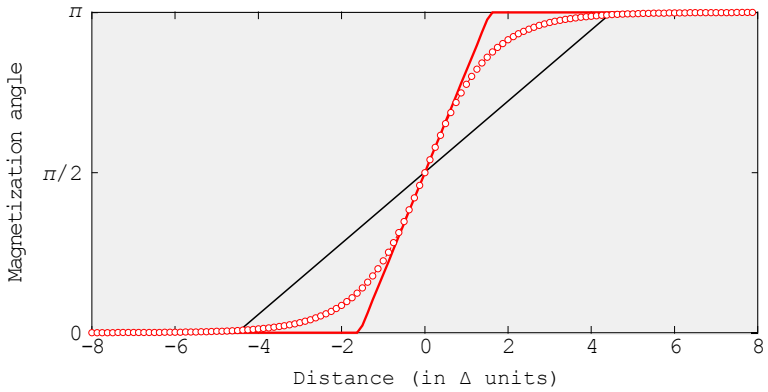

Figure I.9: Bloch domain wall profile: the exact solution (red dots) versus the asymptotic profile (red line). The solution with linear ersatz is shown as a dark line.

By integrating the equations exhibited in the previous section, derive now the exact profile of the domain wall:

$$\theta(x) = 2\arctan[\exp(x/\Delta)] \tag{I.45}$$

and its total energy $\mathcal{E}$.

The most common way to define the Bloch domain wall width δ_{Bl} is by replacing the exact $\theta(x)$ by its linear asymptotes (red line on Figure I.9). To shorten the expressions we often use the notation $\Delta = \sqrt{A/K_u}$, called the Bloch parameter. Derive δ_{Bl} as a function of Δ.

Let us stress two issues:

- The model of the Bloch wall was named after D. Bloch who published this model in 1932[25].
- As often in physics we have seen in this simple example that a dimensional analysis yields a good insight into a micromagnetic situation. It is always worthwhile starting with such an analysis before undertaking complex analytical or numerical approaches, which especially for the latter may hide the physics at play.
- We have exhibited here a characteristic length scale in magnetism. Other length scales may occur, depending on the energy terms in balance. The physics at play will often depend on the dimensions of your system with respect to the length scales relevant in your case. Starting with such an analysis is also wise.
- when the system has a finite size the anisotropy and exchange energy do not cancel at the boundaries. The integration of Euler's equations is more tedious, involving elliptical functions.

Problem 3: Extraction and vibration magnetometer

3.1. Preamble

Here we consider the principle of extraction magnetometry, either in full quasi-dc extraction operation, or in the vibration mode (Vibrating Sample Magnetometer, VSM). Their purpose is to estimate the magnetic moment held by a sample, possibly as a function of field, temperature, time etc. The general principle is to move a sample along the axis of a coil of radius R. This induces a change over time of the flux in the coil, arising from the sample, which may be measured thanks to the induced electromotive force (EMF)[I.11]. In a so-called extraction magnetometer the sample is moved sufficiently away from end to the other along the axis so as to nearly cancel the flux, resulting in an absolute measurement of the flux. In a vibrating sample magnetometer the sample vibrates along the axis at several tens of hertz close to the coil, inducing a large EMF and opening the use of a lock-in technic to further reducing the noise, however the full extraction curve is not measured, resulting in higher sensitivity to artefacts, as will be discussed below.

3.2. Flux in a single coil

Based on the Biot and Savart formula, express as a vector the induction $B(z)$ arising along the axis of a circular coil of radius R with electrical current I. Below is reminded the Biot and Savart formula expressing at an arbitrary location M in space the infinitesimal induction δB arising from a current I on an infinitesimal element δl at location P :

$$\delta B = \frac{\mu_0 I \delta \mathbf{l}(P) \times \mathbf{PM}}{4\pi PM^3} \tag{I.46}$$

For reaching a high sensitivity the coil is wound several time, $N \gg 1$. In the following we will assume $N = 1000$ for numerics. We will assume here that the location of all loops is the same. Based on the reciprocity theorem for induction, derive the magnetic flux $\Phi(z)$ in the series of coils, arising from a pinpoint magnetic moment μ located on the axis of the coil. $\Phi(z)$ will be expressed as $\Phi(z) = Kf(z)$, with $f(z)$ a dimensionless function. Draw a schematics of $f(z)$

Numerics: what is the uniform magnetic induction that would be required to create a flux in these coils, equivalent to that of a square piece of thin film of iron of lateral size 1 cm and thickness 1 nm (reminder: the magnetization of iron is $\approx 1.73 \times 10^6$ A/m). Comment with respect to the magnitude of the earth magnetic field.

3.3. Vibrating in a single coil

The sample is now moved periodically along the axis of the coil, around the location z_0: $z(t) = z_0 + \Delta z \cos(\omega t)$. Based on a first-order expansion in $\Delta z/z_0$,

[I.11] An alternative and very sensitive device for measuring the flux through a coil is SQUID: Superconducting Quantum Interference Device

derive the EMF $e(t)$ induced in the coil. Draw a schematics of this curve. At which position is found the maximum of magnitude for $e(t)$?
Numerics: calculate the magnitude of $e(t)$ arising from the iron thin film mentioned above with a frequency of 30 Hz and $\Delta z = 1$ mm. Comment about this value.

3.4. Noise in the signal

Owing to a mechanical coupling the coils for measurement vibrate with angular frequency ω in the supposedly static induction B applied to magnetize the sample. Let us assume that due the coils' imperfections or finite size this induction displays an inhomogeneity ΔB at the spatial scale for vibration of the sample. Derive the EMF induced in the measuring coils due to this inhomogeneity.
Numerics: vibration of magnitude 1 μm in an induction of strength 1 T, with a relative change of 10^{-3} over a distance of 5 mm. Comment the value.

3.5. Winding in opposition

The above noise can be reduced by using two coils with same axis, measured in series however wound in opposite senses (Figure I.10). The measured EMF is then $e_{\text{tot}}(t) = e_2(t) - e_1(t)$, and the sample is vibrated at equal distance from the two coils, at the position z_0 such that the signal is maximum (see above). Why is the above noise significantly reduced? Comment this setup with respect to the Helmoltz geometry for two coils.

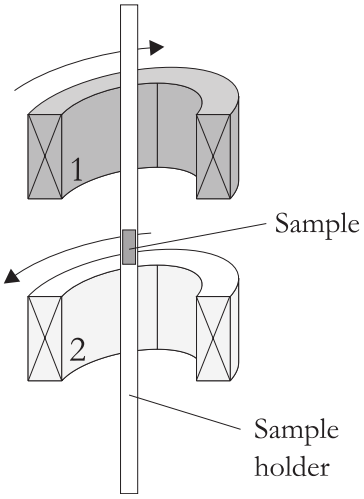

Figure I.10: Geometry for two coils winded in opposite directions

Problem 4: Magnetic force microscopy

This problem is an extension of the short paragraph about magnetic force microscopy in this chapter. This paragraph should be read first, before addressing this problem.

4.1. The mechanical oscillator

The dynamics of the AM cantilever is modeled by a mechanical oscillator:

$$m\frac{\mathrm{d}^2 z}{\mathrm{d}t^2} + \Gamma\frac{\mathrm{d}z}{\mathrm{d}t} + k(z - z_0) = F(z,t) \tag{I.47}$$

$F(z,t)$ is a force arising from either the operator or from the tip-sample interaction, and z_0 is the equilibrium position without applied force. m, Γ and k are the oscillator mass, damping and stiffness, respectively. We use the notation $\omega_0 = \sqrt{k/m}$ and $Q = \sqrt{km}/\Gamma$, the latter being called the quality factor.

Rewrite Eq. (I.47) with the use of ω_0 and Q. The cantilever is excited by the operator with $F(t) = F_{\text{exc}}e^{j\omega t}$. Provide the transfer function $H = z/F$, the gain $G = |H|$ and phase shift $\varphi = \arg(H)$, as well as the following quantities, at resonance: angular velocity ω_{r}, magnitude z_{r} and phase φ_r. For the case $Q \gg 1$ calculate the

magnitude at resonance, and the full-width at half maximum (FWHM) $\Delta\omega_\mathrm{r}$ of the resonance peak. Comment.

4.2. AFM in the static and dynamic modes

The cantilever is brought in the vicinity of the surface, inducing a non-zero force $F(z)$ between the tip and sample, adding up to the sinusoidal from the operator. For the sake of simplicity we will model the variations of F using a simple affine function: $F(z) = F(z_0) + (z - z_0)\partial_z F$.

Calculate the new position at equilibrium z_eq. Rewrite Eq. (I.47) in this case, and in the case $Q \gg 1$ the normalized change of resonance angular velocity $\delta\omega_\mathrm{r}/\omega_0$. In most cases the cantilever is excited at a constant frequency ω_exc and the force gradient is monitored through the change of frequency $\Delta\varphi$. Show that $\Delta\varphi = (Q/k)\partial_z F$.

4.3. Modeling forces

We assume here that the magnetization configurations of both the tip and the sample are not influenced one by another. The vertical component of the force applied by the sample on the tip is $F = -\partial_z \mathcal{E}$, where $\mathcal{E}$ is the mutual energy. The tip may be modeled either by a magnetic dipole $\boldsymbol{\mu}$, or by a magnetic monopole q) (in practice tips may be modeled by a linear combination of both components). For both models express to which z derivative of the vertical component of the sample stray field $H_{\mathrm{d},z}$ are proportional the deflection in the static AFM mode, and the frequency shift in the dynamic AFM mode.

Numerical evaluation – A typical MFM cantilever has $Q = 1000$ and $k = 4\,\mathrm{N/m}$. Modeling both the tip and samples by a magnetic dipole made of Co with a diameter 25 nm, and assuming a probing distance of 50 nm, provide a crude estimate of the frequency shift expected. Comment.

Chapter II

Magnetism and magnetic domains in low dimensions

1 Magnetic ordering in low dimensions

1.1 Ordering temperature

The main feature of a ferromagnetic body is spontaneous ordering below a critical temperature T_C, called Curie temperature. It was Weiss who first proposed a mean-field approach to describe the ordering. In this theory it is postulated that the local moments feel an internal magnetic field

$$\mathbf{H}_i = n_W \mathbf{M}_s + \mathbf{H} \tag{II.1}$$

where $\mathbf{H}$ is the external field, and $n_W \mathbf{M}_s$ is the co-called *molecular field*. This is a phenomenological representation of magnetic exchange, whose quantum-mechanical origin was not known at the time. A semi-classical description allows to link the Heisenberg hamiltonian $\hat{\mathbf{H}} = -2\sum_{i>j} J_{i,j} \hat{\mathbf{S}}_i . \hat{\mathbf{S}}_j$ with n_W:

$$2ZJ_{i,j} = \mu_0 n_W n g_J^2 {\mu_B}^2 \tag{II.2}$$

where Z is the number of nearest neighbors, n the volume density of sites, each holding a dimensionless spin S bounded between $-J$ and $+J$, associated with total magnetic moment $\mu_J = g_J J \mu_B$[II.1]. Based on the site susceptibility related to the Brillouin function$\mathcal{B}_J$, the expected ordering temperature may be expressed as:

$$T_C = \frac{2ZJ_{i,j}J(J+1)}{3k_B} \tag{II.3}$$

The expected Curie temperature is therefore proportional to Z. Let us now draw trends for the Curie temperature in low dimensions. To do this we consider a thin film as a model system, and extend the mean-field approach to averaging the number of nearest neighbors over the entire system. For a film with N layers of sites with magnetic moments we get: $Z_N = Z + 2(Z_s - Z)/N$ where Z_s is the number of nearest neighbors of each of the two surface/ interface layers (Figure II.1a). As $Z_s < Z$ we immediately see based on Eq. (II.3) that the ordering temperature should

[II.1] Beware of this local possible confusion between the exchange constant J, and the total angular momentum J.

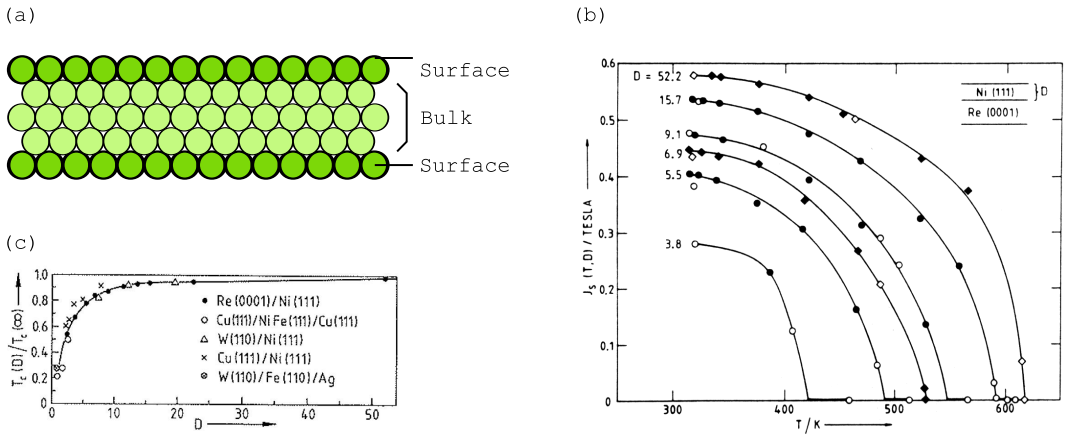

Figure II.1: Magnetic ordering in low dimensions, here with $N = 5$ atomic layers. (a) Counting the reduced average number of nearest neighbors in a thin film with N atomic layers. Example of an experimental determination of (b) the temperature dependence of magnetization and (c) the Curie temperature in various ultrathin film materials[27].

be reduced with a $1/t$ law. Our handwavy considerations are confirmed by a more rigorous layer-dependent mean-field theory[26]. Going beyond mean-field, one may find other critical exponents λ for $T_C \sim t^{-\lambda}$. .

As a rule of thumb, following Eq. (II.3) T_C should be decreased to half the bulk ordering temperature for N equaling one or two atomic layers. Figure II.1b-c shows the $M_s(T)$ variation and the Curie temperature measured for several types of ultrathin films, where the latter prediction appears largely valid, although the scaling law is best fitted with $\lambda = 1.27 \pm 0.20$.

Finally, the $M_s(T)$ law again depends on the model used (dimensionality, type of moment, ordering model), and so do critical exponents in both limits of $T \to 0^+$ and $T \to {T_C}^-$. In the low temperature range the decay is dominated by spin waves and follows a Bloch law:

$$M_s(T) = M_s(T = 0\,\mathrm{K_u})[1 - b_N T^{3/2}] \tag{II.4}$$

whereas mean-field theory predicts an exponentially-weak decay. b_N is the spin-wave parameters, which again happens to be thickness-dependent and well fitted with a $1/t$ law[27]. The case of a truly two-dimensional system should clearly be treated on a different footing due to the absence of out-of-plane excitations. While Onsager derived an expression for the finite Curie temperature in a $2d$ array of Ising spins[28], the Mermin and Wagner theorem states that long-range ordering is not expected to occur at finite temperature for a 2D array of Heisenberg spins; the divergence of susceptibility is found only for $T \to 0\,\mathrm{K}$. This problem has long excited experimentalists, with no report of absence of ferromagnetism in a $2d$ system. The reason is that an energy gap is opened in the spin-wave spectrum as soon as magnetic anisotropy sets in, of magnetocrystalline origin[29] or even simply magnetostatic[30].

Said in a handwavy fashion, any source of anisotropy mimics Ising spins at sufficiently low temperature, going in the direction of the Onsager solution.

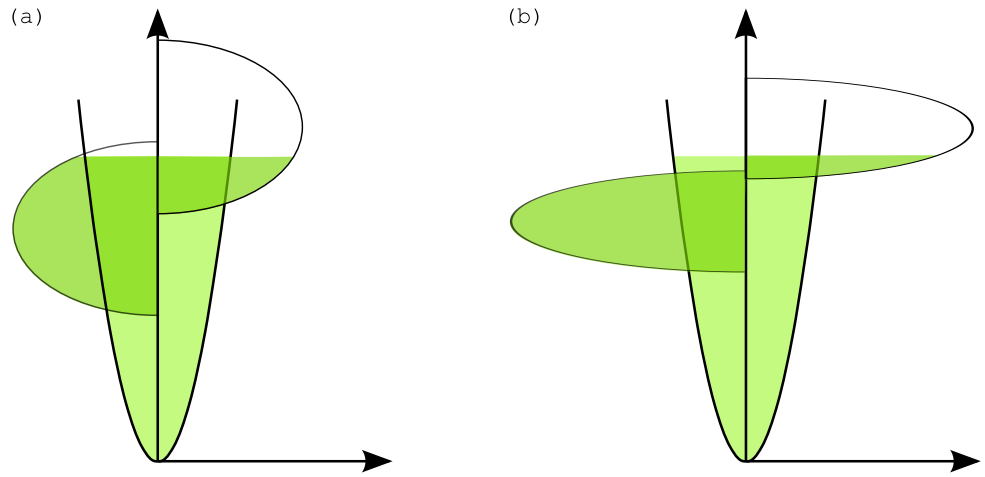

Figure II.2: Schematics of the effect of band narrowing on Stoner criterium and the magnitude of the magnetic moment.

In one dimension thermal fluctuations have an even stronger impact, leading to absence of ordering at any finite temperature even for Ising spins. Thus the correlation length is not expected to diverge until truly zero temperature. Experimental results pertaining to such systems is available and indeed points at the existence of finite-size spin blocks[31].

1.2 Ground-state magnetic moment

Here we discuss the magnitude of the ground-state spontaneous magnetization at zero temperature. The case of itinerant magnetism in $3d$ metals is particularly well documented, and the general trend is physically interesting. Let us consider the case of a free-standing layer, *i.e.* with no supporting nor capping material. Due to the loss of coordination at both surfaces, $3d$ bands are expected to narrow (Figure II.2). As the total number of electrons is conserved this should help satisfying Stoner criterium $I\rho(\epsilon_F)$ where I is the exchange integral and $\rho(\epsilon_F)$ the density of electrons for each spin channel. This in turn should enhance the imbalance of the number of occupied states in both spin channels, and thus magnetization. This trend may be understood as moving towards free electron magnetism were Hund's rules apply and orbital momentum is not quenched, hence giving rise to a larger magnetic moment per atom. In most systems this trend is confirmed through *ab initio* calculations and observed experimentally[27]. Exceptions (reduction of moment with respect to the bulk) may be explained by phenomena whose consequences are more difficult to predict such as epitaxial or surface strain, dislocations, hybridization and charge transfer with an interfacial material, quantum-size effects.... Mainly the latter play a role in more localized magnetism, leading to effects more difficult to predict.

Thin films are easy to model and simulate thanks to translational invariance. However low-dimensional effects arise equally in other systems such as clusters. The magnetic moment per atom has been measured to be clearly enhanced in these, evidenced in-flight with Stern-Gerlach experiments or capped with sensitive techniques such as XMCD[32]. The Stoner criterium may even be fulfilled in clusters, while it is not in the bulk form. A famous case is Rhodium[33, 34].

Conclusion

We have reviewed the basics of ferromagnetic ordering in low dimensions for itinerant magnetism. The general trend is that of two competing effects. The zero-temperature ground state displays a moment generally larger than that of the bulk, due to band narrowing. An opposite trend if the enhanced *decay* of magnetization with temperature. At finite temperature both effects compete, requiring care in the analysis of measurements.

2 Magnetic anisotropy in low dimensions

We first consider magnetostatic anisotropy, long-ranged and related to the outer shape of a system. We then consider the magnetic anisotropy of microscopic origin, arising from spin-orbit and the crystal electric field. These are magnetocrystalline and magnetoelastic anisotropies, which were introduced in sec.3. We consider thin films as a model system, however those concepts apply to all low-dimensional systems, however in a more complex manner.

2.1 Dipolar anisotropy

In sec.4.3 we introduced the concept of demagnetizing factors. These were calculated on the assumption that the system under consideration is uniformly magnetized. Although this may be questionable in some cases even under applied field, in the present section we will rely on these factors for a first discussion. In this framework we have seen [Eq. (I.25)] that the dipolar contribution to magnetic anisotropy reads, after proper diagonalization defining the so-called main directions of anisotropy: $E_\mathrm{d} = -K_\mathrm{d} N_i m_i$, and the internal so-called demagnetizing f477ield reads $\mathbf{H}_\mathrm{d} = -N_i M_i \mathbf{u}_i$, where i runs over all three main directions, and $N_x + N_y + N_z = 1$.

For thin films $N_x = N_y = 0$ along the two in-plane directions, resulting in zero demagnetizing field and demagnetizing energy. N_z=1, resulting in $E_\mathrm{d} = K_\mathrm{d}$ and $\mathbf{H}_\mathrm{d} = -M_\mathrm{s}\mathbf{u}_z$ for perpendicular magnetization. The resulting demagnetizing induction $\mu_0 M_\mathrm{s}$ is of the order of one Tesla for common materials (Table I.2).

Unless the material displays a very large microscopic energy, or a very strong field is applied perpendicular to the plane, the magnetization of a thin film lies preferentially in-the-plane.

For cases other than films, however of reduced dimension in at least one direction, we will speak of nanostructures. The demagnetizing factors are all three non-zero, and again if no microscopic energy or applied field applies, the magnetization will have a tendency to point along the direction with the lowest demagnetizing factors.

Let us add a fine point often subject to controversy, however of great importance for domains and magnetization reversal in nanostructures: the range of dipolar interactions. Dipolar interactions are commonly described as long-ranged. This is so because the stray field from a magnetic dipolar decays with distance like $1/r^3$. Thus, an upper bound for the stray field at a given location is of type $\int (1/r^3) 4\pi r^2 \mathrm{d}r$, summing over the entire system magnitudes instead of vectors. This diverges logarithmically (however converges if vectors are considered instead of magnitudes),

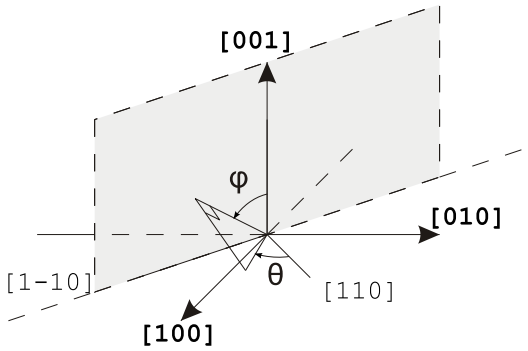

Figure II.3: Definition of axes for a cubic crystal projected along the (110) plane.

revealing the long range of dipolar fields. More precisely, it is straightforward to show that what matters is the solid angle under which a surface density of charges is seen, not its distance. Let us now consider a flat system, for instance an element patterned out of a thin film with lithography. The upper bound becomes $\int(1/r^3)2\pi r dr$, which converges to a finite value with a radius of convergence scaling with the sample thickness. In other words:

Dipolar energy is short-ranged in two dimensions. This can be understood in a handwavy manner as most stray field escapes in the third dimension, not contributing to the self energy $-(1/2)\mu_0\mathbf{M}_s\mathbf{H}_d$. This implies that stray- and demagnetizing fields are often highly non-homogeneous, with important consequences on both magnetization patterns and magnetization reversal processes. For the same reason, the concept of demagnetizing factors and shall be used with great care in such cases

Elements with two flat surfaces (made out of a thin film) and with a circular or ellipsoid shape are not ellipsoids. Their demagnetizing field is therefore highly non-uniform, as for all flat elements.

2.2 Projection of magnetocrystalline anisotropy due to dipolar energy

One consequence of magnetostatic energy is to favor the alignement of magnetization in directions with small demagnetizing coefficients. If magnetostatic energy prevails over magnetocrystalline anisotropy energy, the magnetization will tend to lie in certain planes or directions imposed by the former, while the latter will play a role only through its projection in these planes or directions. Let us consider the example of a cubic material; its magnetocrystalline anisotropy is described by Eq. (I.8), whose magnitude is measured through the parameter K_{1c}. If K_{1c} is much smaller than K_d then the direction of magnetization will be imposed by the latter, for instance in-the-plane for a thin film (sec.4.3). As an example, let us consider a cubic crystal cut along a (110) plane (Figure II.3). When restricted to $\varphi = 90°$, Eq. (I.8) reads:

$$E_{\mathrm{mc,cub}} = K_{1c}\sin^2\varphi + (-\frac{3}{4}K_{1c} + \frac{1}{4}K_{2c} + K_{3c})\sin^4\varphi + \dots \qquad \text{(II.5)}$$

Then, the effective anisotropy in the plane becomes uniaxial.

We illustrated a feature of symmetries with application to many fields in physics, such as bulk versus surface crystallography: considering of a function defined in a space with d dimensions and displaying certains symmetries, its projection or restriction into a sub-space of dimension lower than d does not necessarily preserve or restrict the initial symmetry, even if the sub-space is an element of symmetry of the initial function.

2.3 Interface magnetic anisotropy

The local environment of atoms differs at both surfaces of a thin film with respect to the bulk one. In 1954 L. NÉEL suggested that this breaking of symmetry induced by the loss of translational invariance along the normal to the film, should result in an additional term to magnetic anisotropy. This was well before technology enabled to produce films so thin and well characterized that experiments could suggest the effect. This additional term is called *surface magnetic anisotropy*, or *interface magnetic anisotropy*, or also *Néel magnetic anisotropy*[II.2].

As for magnetocrystalline anisotropy, interface anisotropy may favor an easy direction or an easy plane, and be decomposed in angular terms with various orders. As it applies only once per each interface, its effects becomes vanishingly small at large thickness. In practice it is observed that its effect becomes negligible beyond a few nanometers. One speaks of ultra thin films in this range smaller than characteristic length scales, where magnetization is obviously allowed to vary along the thickness. At a given lateral position its magnetization[II.3] may be described as a single vector, the so-called macrospin, on which apply both surface and bulk magnetic anisotropy. As a simple example let us assume that both terms are uniaxial along the same axis, with two identical surfaces. The resulting anisotropy then reads $K_{\mathrm{v}}t + 2K_{\mathrm{s}}$ with K_{v} and K_{s} the volume and surface contributions. The effective density of energy thus reads:

$$K_{\mathrm{eff}} = K_{\mathrm{v}} + \frac{2K_{\mathrm{s}}}{t} \tag{II.6}$$

Following this, the usual way to estimate K_{s} in theory and experiments is to plot K_{eff} versus $1/t$. The intercept with the y axis should yield the bulk anisotropy, while the slope should yield K_{s} (Figure II.4). Interfacial anisotropies between various types of materials has thus been tabulated[27, 36]. K_{s} indeed depends on the material, may be of different sign, and is of the order of $0.1\,\mathrm{mJ.m^{-2}}$.

In its 1954 model Néel proposed the estimation of an order of magnitude for K_{s} values, based on the phenomenological analogy between removing the atoms to create an interface, and pulling them away infinitesimally. K_{s} was then linked with magneto-elastic constants of the material, with surprisingly a good agreement on the order of magnitude, although the exact value and even the sign may be wrong. The so-called *pair model* of Néel aims at describing the direction and material-

[II.2] In principle interface is appropriate to describe a thin magnetic film in contact with another material while surface is appropriate to describe a free surface (in contact with vacuum). This latter case is in principle restricted to fundamental investigations performed *in situ* in UHV, where a surface may remain free of contaminant for some time. In practice, both terms are often used interchangeably

[II.3] More precisely its moment per unit area, thus expressed in Amperes

dependence of surface anisotropy by counting the bounds between a surface atom and the neighbors, and associate them with a uniaxial angular function.

Theory can also be used to evaluate K_s values. Letting aside *ab initio* calculations, for $3d$ metals tight binding links magnetocrystalline anisotropy with the anisotropy or the orbital magnetic moment. For a uniaxial anisotropy the energy per magnetic atom is:

$$\kappa = \alpha \frac{\xi}{4\mu_B} \Delta\mu_L. \qquad \text{(II.7)}$$

ξ is the spin-orbit coupling, defined by contribution $-\xi \hat{\mathbf{S}}.\hat{\mathbf{L}}$ to the Hamiltonian. $\Delta\mu_L$ is the difference of orbital magnetic moment between hard and easy directions, and α is a factor close to unity and only weakly related with the details of the band structure.

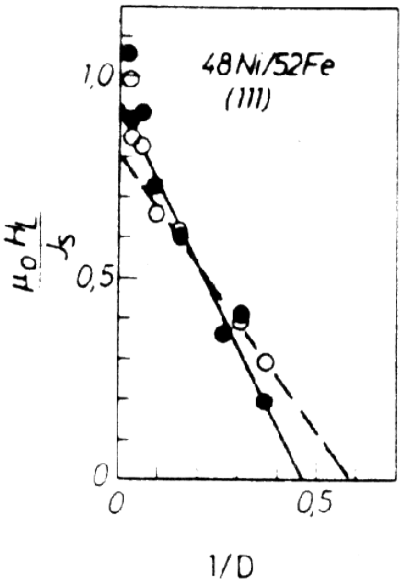

Figure II.4: A historical example of $1/t$ plot for evaluating interfacial anisotropy[35].

In bulk $3d$ metals the orbital momentum is nearly fully quenched because crystal electric field energy dominates over spin-orbit, and eigen functions in a cubic symmetry should have nearly zero orbital momentum. Thus $\Delta\mu_L$ are very weak, typically of the order of $10^{-4}\,\mu_B$/atom, yielding $K \approx 10^4\,\mathrm{J/m^3}$. At both surfaces and interfaces this anisotropy is enhanced close to $0.1\,\mu_B$/atome, inducing an anisotropy of energy of the order of 1 meV per surface atom, which lies close to $1\,\mathrm{mJ/m^2}$. The link between surface magnetic anisotropy and $\Delta\mu_L$ has been checked experimentally and by *ab initio* calculations to be essentially valid. Some experiments hint at a quantitative link between bulk and surface magnetic anisotropy[37], however the universality of this link remains speculative.

The most dramatic consequence of surface magnetic anisotropy, with also of technological use, arises when K_s favors the alignement of magnetization along the normal to a thin film : $E_s = K_s \cos^2(\theta)$ with $K_s < 0$ and θ the angle between magnetization and the normal to the film. If Eq. (II.6) is negative and becomes greater in absolute value than K_d for a realistic critical value of thickness t_c, magnetization will point spontaneously along the normal to the film. This is perpendicular magnetic anisotropy (PMA). For a long time the most efficient interfaces to promote PMA combined $3d$ elements for the ferromagnet, and a heavy element to bring in spin-orbit. Prototypical examples are Co/Au, Co/Pt and Co/Pd. t_c is of the order of 2 nm or less. Recently even larger contributions to perpendicular anisotropy, and thus larger critical thicknesses (up to 3.5 nm), have been reported at the interface between 3d metals and oxides, with the prototypical case of Co/MgO. If films thicker than this are needed with perpendicular magnetization, a route is the fabrication of multilayers[36].

2.4 Magnetoelastic anisotropy

The concept of magnetic surface anisotropy has been presented above as a textbook case. In fact it is not the single source of modification of magnetic anisotropy in ultrathin films. We review here an equally important source, magnetoelastic anisotropy.

In the bulk form strain may be obtained through stress applied by an external user. Strain is always present in thin films to some extent even at rest. This is due to the effect of the supporting material (and to some smaller extent the capping material), which having a lattice parameter and possibly symmetry different from that of the overgrown magnetic material, stresses the latter. Stress may also appear upon cooling (resp. warming up) thin films fabricated at high (resp. low) temperature. This results in a strain field in the magnetic film, generally not uniform, which gives rise to a magnetoelastic contribution to the total MAE.

One should not confuse strain with stress. The former is the deformation, the latter is the force related to the strain.

To first order magnetoelastic anisotropy is proportional to the matrix elements of strain. Group theory predicts the type of coupling terms[38], not their strength. In thin films there clearly exists an asymmetry between out-of-plane and in-plane directions: stress is applied in the latter, while along the former the film is free to relax. This results in a uniaxial magnetoelastic contribution.

Let us understand the qualitative effect of magnetoelasticity in thin films using a simple model. We consider the epitaxial growth of a film material (lattice parameter a_f) on a substrate (lattice parameter a_s), the latter being assumed to be rigid. The lattice misfit is defined as $\eta = (a_\mathrm{f} - a_\mathrm{s})/a_\mathrm{s}$. During growth the deposited material will tend to relax its strain $\epsilon = (a - a_\mathrm{f})/a_\mathrm{f}$ through, *e.g.*, the introduction of interfacial dislocations. We further assume that the linear energy cost per dislocation k does not depend on the density of dislocations, and that each dislocation allows the coincidence of $N+1$ atoms of the film with N substrate atoms (resp., the reverse), which corresponds to negative (resp. positive) η. Working in a continuum model, the density of mechanical energy of the system is :

$$E_\mathrm{mec} = \frac{1}{2} C\epsilon^2 + \frac{k}{t a_\mathrm{f}} |\eta + \epsilon - \epsilon^2| \tag{II.8}$$

where t is the film thickness and C a elastic constant. The equilibrium value for a is found through minimization of this equation with the constraint $|\epsilon| < |\eta|$:

- Below the critical thickness $t_\mathrm{c} = k/(a_\mathrm{s} C|\eta|)$ the introduction is dislocation is unfavorable, and $a = a_\mathrm{s}$. The layer is said to be pseudomorph. As a rule of thumb, $t_\mathrm{c} \approx 1\,\mathrm{nm}$ for $\eta \approx 2 - 5\,\%$. This value is however dependent on the crystal symmetry, growth temperature and technique of deposition.
- Above e_f dislocations are created and reduced strain, following: $|\epsilon(e)| = k/(a_\mathrm{s} C t)$.

What what have described so far is a structural model, proposed in 1967 by Jesser[39]. In 1989 Chappert et Bruno applied this model to magneto-elasticity[40].

They considered linear magneto-elastic terms[II.4]. As a simple case, let us assume that all deformations may be expressed in terms of ϵ, so that $E_{\text{mel}} = B\epsilon$ with B a coupling constant. Based on the structural model of Jesser we derive: $K_{\text{mel}} = kB/(a_{\text{s}}Ct)$. Beyond the pseudomorphic regime we therefore expect a dependence of K_{mel} with $1/t$, thus exactly like for a contribution of magnetic interface anisotropy. In most cases magneto-elasticity and surface anisotropy are intermingled in thin films; it is almost impossible experimentally and conceptually to disentangle them. Nevertheless, it remains common to designate as *surface anisotropy* the total effective contribution revealed as a $1/t$ variation of the density of magnetic anisotropy.

2.4.a Anisotropy resulting from the synthesis process

Following the above, it might be expected that beyond a few nanometers of thickness, the anisotropy of thin films is similar to that of bulk. While this is often the case, there are cases of persistence for large thickness of a magnetic anisotropy different from the bulk one.

A first reason is the the Jesser model considers the minimum of energy. In practice this minimum may not be reached perfectly due to the energy barriers required to create dislocations, and it is often the case that thin films retains a fraction of percent if strain. The exact value strongly depends on the couple of materials, the orientation of the grains, the conditions and technic of deposition.

A second reason for the persistence of deviations from bulk anisotropy is the often fine microstructure induced by the growth method. The microstructure may take the form of grains separated by grains boundaries, incorporated of foreign atoms (like Ar during sputtering growth), an anisotropic orientation of atomic bounds etc. This effect has dramatic consequences for materials with large magnetostriction such as 3d-4f compounds, which can be tailored to display perpendicular anisotropy for fairly thick films. It is also possible to tailor a uniaxial anisotropy between two in-plane directions, through deposition under an applied field like for Permalloy ($Ni_{80}Fe_{20}$), or deposition with oblique incidence or on a trenched surface. Another elegant technique to tailor the anisotropy of thin films is irradiation with ion of medium energy. This irradiation may be done during growth or post-growth. When the irradiation energy is suitably chosen, the ions may either favor the mixing of atoms or their segregation, depending on the thermodynamics trend for alloying on phase separation. Irradiating thin films with perpendicular anisotropy, the former leads to a decrease of anisotropy, while the latter leads to an increase. Irradiation may be combined with masks to deliver films with patterned anisotropy, however no changes in topography[42].

Conclusion

Contributions to magnetic anisotropy of energy in thin films include magnetostatic, magnetocrystalline, interfacial and magnetoelastic energies. For very thin films the latter two often dominate in the nanometer range of thickness, opening the way to beating dipolar anisotropy to display perpendicular magnetization.

[II.4] It was recently shown that non-linear effects may be important in thin films[41]. This effect had not been reported in bulk materials, where plastic deformation sets in well before strain values large enough for non-linearities may be reached

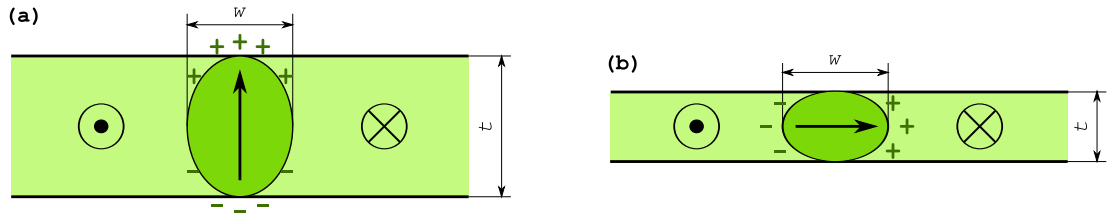

Figure II.5: Schematics for (a) a Bloch domain wall and (b) a Néel domain wall.

3 Domains and domain walls in thin films

3.1 Bloch versus Néel domain walls

In sec.6.5.csec.?? we considered a textbook case of domain-wall: the Bloch domain wall, resulting from the competition of exchange energy against magnetocrystalline anisotropy. A translational invariance along both directions perpendicular to the domain wall was assumed, so that the problem boiled down to a unidimensional equation that can be solved.

Translational invariance makes sense in the bulk, where domain walls may extend laterally on distances much longer than their width. This hypothesis becomes questionable in thin films, where the core of a Bloch domain wall, displaying perpendicular magnetization, induces the appearance of magnetic charges at both surfaces of the thin film (Figure II.5a).

L. NÉEL was first in addressing this issue and providing a rule-of-thumb prediction for a cross-over in the nature of domain walls in thin films[43]. In a thin film of thickness t he considered a domain wall of bulk width $w \approx \Delta_u$, such as determined from exchange and anisotropy energies. He took into account the finite size effect along the normal to the film, modeling the domain wall as a cylinder of perpendicular magnetization with an elliptical cross-section of axes $w \times t$ (Figure II.5). For a Bloch domain wall the resulting density of magnetostatic energy is $K_d \; w/(w+t)$, based on demagnetizing coefficients (Table I.3). When $t < w$ it becomes more favorable for magnetization in the core of the domain wall to turn in-the-plane, for which the density of magnetostatic energy is $K_d \; t/(w+t)$ (Figure II.5b). This configuration where magnetization turns in-the-plane, *i.e.* perpendicular to the domain wall, is called a Néel wall.

In the above model the core of the domain wall was assumed to be rigid and uniformly magnetized. Besides, its energy was calculated crudely, and is not suitable for soft magnetic materials where magnetostatic energy dominates magnetic anisotropy so that no natural width of the domain wall exists. The phase diagram of Bloch versus Néel wall can then be refined using micromagnetic simulations. These show in the case of soft magnetic material that Néel walls become stable for thickness below $7\Delta_d$ (already below $15-20\Delta_d$ for cross-tie walls, see next paragraph) *e.g.* for 50 nm for Permalloy and 20 nm for Fe[44].

Micromagnetic simulations also revealed a phase diagram more complex than merely Bloch versus Néel walls (Figure II.6a). Going towards large thicknesses domain walls undergo a breaking of symmetry with respect to a vertical plane; they are named asymmetric Néel wall and asymmetric Bloch wall, and were first proposed in 1969 through both micromagnetic simulation[45] and an ersatz model[46]. Let us

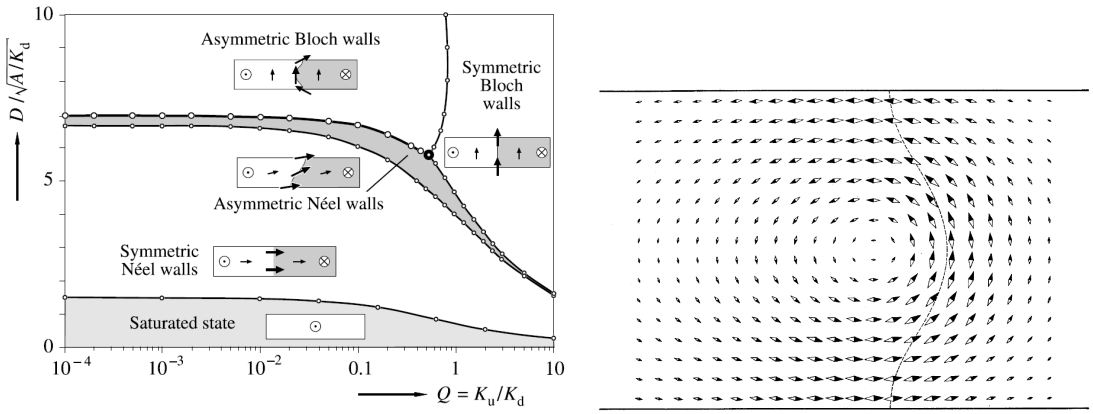

(a) (b)

Figure II.6: (a) phase diagram of domain walls in thin films, calculated for practical reasons in a stripe of finite width[44] (b) one of the first success of micromagnetic simulation, predicting the existence of the asymmetric Bloch domain wall[45].

examine the detail of the asymmetric Bloch wall, of higher practical interest (Figure II.6b). Close to the surface the magnetization turns in-the-plane; this may be understood from the necessity to eliminate surface magnetic charges to decrease magnetostatic energy, or in other words to achieve a flux-closure state. The surface profile of magnetization is similar to that of a Néel wall, later motivating the name of Néel cap do designate this area of flux-closure[47]. Notice that the center of the Néel cap is displaced from the vertical of the core of the Bloch wall, explaining the name asymmetric for this domain wall. This asymmetry arises so as so reduce now volume magnetic charges, balancing $\partial_x m_x$ with $\partial_z m_z$ terms in the divergence of $\mathbf{M}$. Close to the transition from Bloch to Néel the cross-section of the asymmetric Bloch wall looks similar to a vortex, so that the name vortex wall is sometimes used.

3.2 Domain wall angle

We define as wall angle θ, the angle between the direction of magnetization in two neighboring domains. The properties of a domain walls as a function its angle depend on parameters such as film thickness t, anisotropy strength and symmetry. Here we restrict the discussion to rather soft magnetic materials in rather thin films, so that most of the energy of a domain wall is of magnetostatic origin.

The density of volume charges in an extended domain wall is $-\partial_x M_x$, where x is the coordinate along the in-plane axis perpendicular to the domain wall (Figure II.7). Generally a wall is induced to bisect the direction of magnetization of the two neighboring domains, so that is bears no net magnetic charge and thus does not contribute significantly to magnetostatic energy through a long-range $1/r$ decay of stray field (Figure II.7). Following Néel, we model the core of the domain wall with a cylinder of elliptical cross-section, and estimate its energy through the suitable demagnetizing coefficient.

We first consider a Néel wall. The total quantity of charge in each half of the elliptical cylinder scales with $1 - \cos(\theta/2)$, which can be replaced with a reasonable accuracy with $\theta^2/8$. As dipolar energy scales with the square of charges, and as-

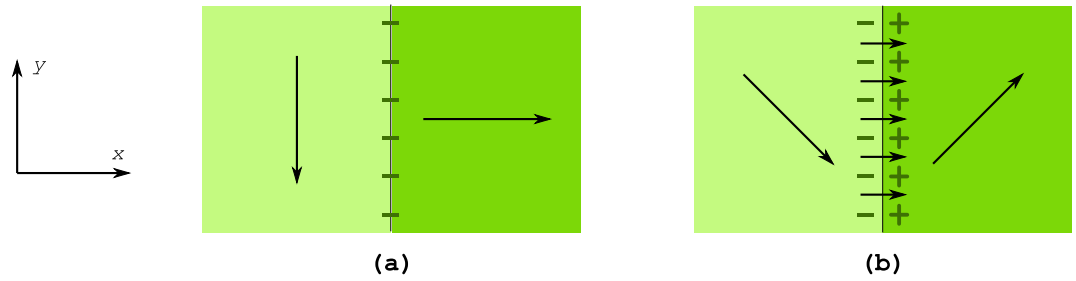

Figure II.7: Wall angle and magnetostatic charges. (a) A wall that would not bisect the direction of magnetization in the neighboring domains would bear a net charge (b) A wall bisecting the magnetization directions in neighboring domains is associated with a dipolar line.

suming that the domain wall width does not depend significantly on the wall angle, we come to the conclusion that the energy of a Néel domain wall varies like θ^4.

We now consider a Bloch wall. Volume charges can be avoided if m_x is uniform and equal to $\cos(\theta/2)$ from one domain to the other, through the domain wall. This means that, apart from the case $\theta = 180°$, the core of such a wall has both in-plane and out-of-plane components, the latter equal to $\sqrt{1-\cos^2(\theta/2)} = \sin(\theta/2)$. Thus the magnetostatic energy a Bloch wall scales like $\sin(\theta/2) \approx \theta^2/4$.

The energy of a domain wall depends on its angle θ. In this films the energy of a Néel wall varies like θ^4, much faster than that of a Bloch wall, varying like θ^2.

3.3 Composite domain walls

Dramatic consequences result from the convex variation of domain wall energy with angle outlined above. To set ideas, the cost per unit length of a 90° Néel wall is less than 10 % that of a 180° Néel wall. This means that a 180° Néel wall may be unstable and be replaced by walls of smaller angle, even is this implies an increase of the total length of domain wall. This is confirmed experimentally with the occurrence of composite domain walls.

One type of composite domain wall is the so-called cross-tie (Figure II.8a-b). It can be checked that each wall fulfils is bisecting the neighboring domains. Cross-tie domain walls occur only in soft magnetic material, because the extended domain with different orientations shall not come at the expense of an anisotropy energy. Notice also that as the energy of a Bloch wall scales like θ^2 whereas that of a Néel scales like θ^4 (see previous paragraph), 180° Bloch walls are replaced with cross-tie walls for a thickness larger than that predicted by the Néel model for the cross-over between Bloch and Néel.

Another type of composite wall is the zig-zag domain wall. Although domain walls tend to bisect the direction of neighboring domains, it may happen due to the history of application of field and nucleation of reversed domains, that two domains face each other and are each stabilized, *e.g.* by a uniaxial anisotropy or a gradient of external field with opposite signs. A 180° is unstable as the net magnetostatic charge carried would be M_s, the largest possible value. In this case the domain wall breaks into short segments connected in a zig-zag line (Figure II.8c-d). Along

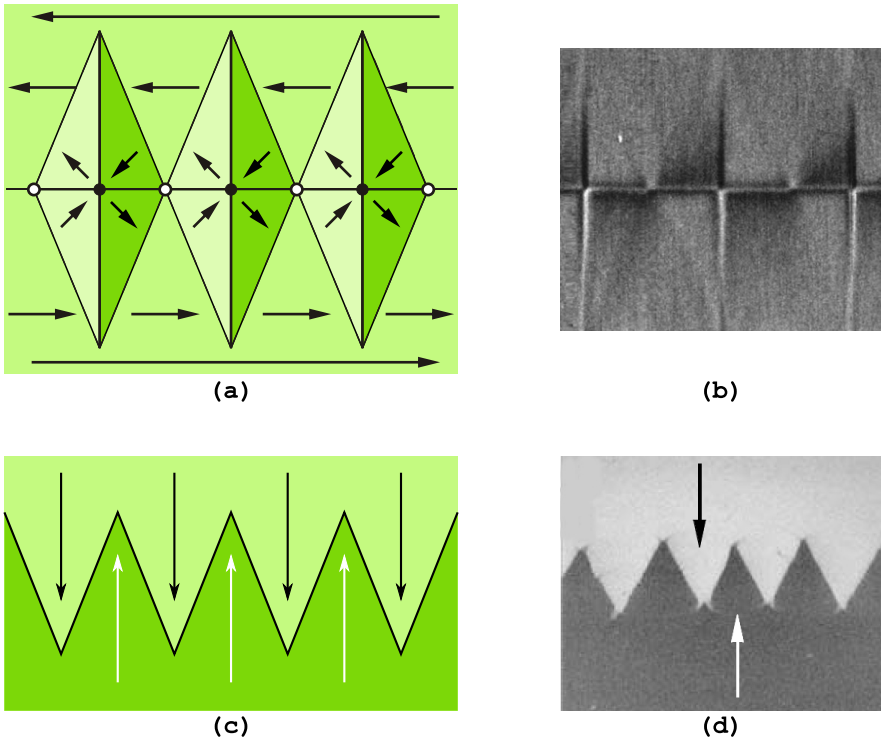

Figure II.8: Composite domain walls in thin films: (a-b) Schematics and MFM image ($13 \times 15\,\mu$m)[48] of a cross-tie wall. On the schematics open and full dots stand for vortices and antivortices, respectively (c-d) schematics and Kerr image($350 \times 450\,\mu$m)[6] of a zig-zag wall.

the segments the walls have a tendency to turn 180° to be free of volume charges, implying some continuous rotation of magnetization in the dihedron formed by two consecutive segments. The angle of the zig-zag is determined by a complex balance between the reduction of magnetostatic energy due to the net charge, versus the increase of energy through the wall length, and anisotropy and exchange energy in the domains.

3.4 Vortices and antivortex

The inspection of Figure II.8a reveals the existence of loci where, from symmetry and continuity arguments, the direction of magnetization may be in no direction in the plane. These were called Bloch lines, consisting of a cylinder of perpendicular magnetization separating two Néel walls with opposite directions of in-plane magnetization. The direction of perpendicular magnetization in a Bloch line is called the polarity, and summarized by the variable $p = \pm 1$. Bloch lines also occur inside Bloch walls, separating parts of the wall core with opposite directions of perpendicular magnetization. Thus Bloch lines are the one-dimensional analogous domain walls, separating two objects of dimensionality larger by one unit. In Bloch lines exchange and dipolar energy compete, yielding a diameter scaling with Δ_d, of the order of 10 nm in usual materials.

It is useful to introduce the concept of winding number defined like:

$$n = \frac{1}{2\pi} \int_{\partial\Omega} \nabla\theta . \mathrm{d}\boldsymbol{\ell} \tag{II.9}$$

where $\partial\Omega$ is a path encircling the Bloch line, and θ is the angle between the in-plane component of magnetization and a reference in-plane direction. Applied to the cross-tie wall, this highlights alternating Bloch lines with $n = 1$ and $n = -1$ (resp. open and full dots on Figure II.8a). The former are also called vortex and the latter anti-vortex. Notice that through the transformation of a translation-invariant Néel wall with no Bloch line into a cross-tie wall, the total winding number is thus conserved. This is a topological property, which will be further discussed in the framework of nanostructures (see sec.4).

We also introduce the chirality number:

$$c = -\frac{\mathbf{k}}{2\pi} . \int_{\partial\Omega} \nabla\mathbf{m} \times \mathrm{d}\boldsymbol{\ell} \tag{II.10}$$

where $\mathbf{k}$ is the normal to the plane defining its chirality. On Figure II.8a) vortices have $c = +1$.

Bloch lines are fully characterized by three numbers: polarity p, winding number n and chirality c. An antivortex has zero chirality, while vortices have $c = \pm 1$ depending on the sense of rotation of magnetization, either clockwise or anticlockwise.

There exists also a zero-dimensional object, the Bloch point, separating two parts of a Bloch line with opposite polarities. For topological (continuity) reasons, at the center of the Bloch point the magnitude of magnetization vanishes, making it a very peculiar object[49].

3.5 Films with an out-of-plane anisotropy

Here we consider thin films with a microscopic contribution to the magnetic anisotropy energy, favoring the direction perpendicular to the plane. Most depends on the quality factor $Q = K_\mathrm{u}/K_\mathrm{d}$ and film thickness t. For $Q < 1$ uniform in-plane magnetization is a (meta)stable state however with large energy, while uniform out-of-plane magnetization is not a (meta)stable state. For $Q > 1$ the situation is reversed. In all cases a balance between anisotropy energy and shape anisotropy needs to be found, the best compromise being through non-uniform states. The competition of all four energy terms leads to a rich phase diagram, see Ref.6 for a comprehensive theoretical and experimental review. A schematic classification with no applied field is presented below, and summarized in Table II.1.

In the case of large thickness (see table and below for numbers), in all cases the state of lowest energy is one of alternating up-and-down domains, with a period $2W$ (Figure II.9a). This pattern is called strong stripe domains. This situation was first examined by Kittel[50], and later refined by several authors. The alternance cancels surface charges on the average, keeping magnetostatic energy at a low level. Magnetic anisotropy is also kept at a low level as most of magnetization lies along an easy direction. The remaining costs in energy arise first from the vertical domain walls (of Bloch type with in-plane magnetization to avoid volume charges), second

Table II.1: Summary of the magnetization state of films with an out-of-plane contribution to magnetic anisotropy. t and W are the film thickness and the optimum domain width, respectively.

	$Q < 1$	$Q > 1$
$t > t_c$	Weak to strong stripe domains with increasing t. $W \sim t^{1/2}$ and then $W \sim t^{2/3}$ upon branching	Strong stripe domains. $W \sim t^{1/2}$ and then $W \sim t^{2/3}$ upon branching. May be hindered by hysteresis.
t_c	Second order transition (no hysteresis in the case of purely uniaxial anisotropy) from uniform in-the-plane to weak stripes	The minimum value for W is reached.
$t < t_c$	Uniform in-plane magnetization	Perpendicular domains with diverging W, however quickly masked by hysteresis.

from flux-closure slabs close to the surface with a complex mixture of anisotropy, dipolar and wall energy. Minimization of this energy yields straightforwardly an optimum value for W scaling like $\sqrt{t}$, more precisely like $\sqrt{t\sqrt{AK_u}/K_d}$ for $Q \gtrsim 1$ (Figure II.9a) and like $\sqrt{t\sqrt{A/K_u}}$ for $Q \lesssim 1$ (Figure II.9b). At quite large thicknesses[6], typically hundreds of nanometers or micrometers, this law is modified due to branching of domains close to the surface (Figure II.9c). Branching decreases the energy of closure domains, while saving wall energy in the bulk of the film. We then have $W \sim t^{2/3}$.

For decreasing thickness we shall consider separately two cases. For $Q > 1$ there exists a critical minimum domain width $W_c \approx 15\sqrt{AK_u}/K_d$, which is reached for $t_c \approx W_c/2$. Below this thickness flux-closure between neighboring domains becomes largely ineffective due to the flat shape of the domains, thereby leading to a sharp increase of W, with ultimately a divergence for $t \to 0$ (Figure II.9d). For $Q < 1$ the magnetization in the domains progressively turns in-the-plane, with a second-order transition towards a uniform in-plane magnetization around $t = 2\pi\Delta_u$. This pattern is called weak stripe domains due to the low angle modulation of direction of magnetization in neighboring domains. Close to the transition $W \approx t$ and the deviations from uniformity are sinusoidal to first order.

In the above, notice that the state with lowest energy may not be reached for $Q > 1$, as the uniform state perpendicular to the plane is (meta)stable. Thus strong stripe domains may not occur even at large thickness, for very coercive materials. Below t_c the energy gain resulting from the creation of domains is very weak, so that the divergence of W is often hidden again behind coercive effects.

Conclusion

The features of domain walls are different in thin films, compared to

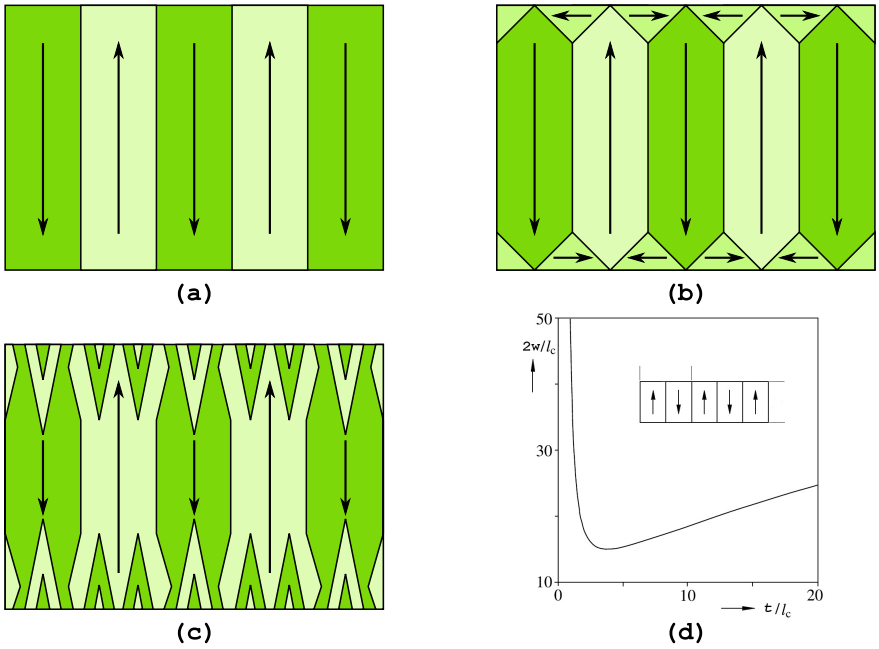

Figure II.9: Stripe domains. Sketches for (a) open domains (initial Kittel's model, (b) perfect flux-closure domains and (c) domain branching. (d) predicted width of domain W with film thickness t, from ref.6. $l_c = 2\sqrt{AK_u}/K_d$

the bulk. This is mostly related to the need to reduce dipolar energy, arising because of the loss of translational invariance along the normal to the film. The thickness of the film has a strong impact, and often approximations are required to describe the physics analytically.

4 Domains and domain walls in nanostructures

In this section we examine the effect of reducing the lateral dimensions of nanostructures, from large to small nanostructures. We consider first the domains, followed by special cases of domain walls.

4.1 Domains in nanostructures with in-plane magnetization

We consider a piece of a thin film of soft magnetic material, quite extended however of finite lateral dimensions. Under zero applied field these assumptions allow us to describe the arrangement of magnetization as an in-plane vector field $\mathbf{m}$ of norm unity, and neglect the energy inside and between domain walls. Under these conditions Van den Berg proposed a geometrical construction to exhibit a magnetization distribution with zero dipolar energy[51, 52]. As dipolar energy is necessary zero or positive, this distribution is a ground state.

Zero dipolar energy can be achieved by canceling magnetic charges. Absence of surface charges $\mathbf{M}.\mathbf{n}$ requires that magnetization remains parallel to the edge of the nanostructure (Figure II.10); this is a boundary condition. At any point P at the border, let us consider the cartesian coordinates (x, y) with x and y respectively tangent and inward normal to the boundary. The density of volume charges reads

$\partial_x m_x + \partial_y m_y$. As **m** lies along x, $\partial_x m_x = 0$. Thus cancelation of volume charges is achieved if $\partial_y m_y = 0$; this is the differential equation to be solved. As $m_y = 0$ at the boundary, absence of volume charges is fulfilled by keeping **m** normal to the radius originating from P.

Radii originating from different points at the boundary may intersect, each propagating inwards magnetization with a different direction, in which case highlighting the locus of a domain wall. It can be demonstrated that domain walls in the nanostructure are at the loci of the centers of all circles inscribed inside the boundary at two or more points. This geometrical construction satisfies that any domain wall is bisecting the direction of magnetization in the neighboring domains, a requirement pointed out in sec.3.2. Figure II.11a-b shows examples of the Van den Berg's construction. A mechanical analogy of this construction is sand piles, where lines of equal height stand for flux lines.

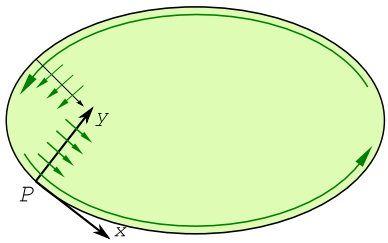

Figure II.10: The principle for building a magnetizaiton configuration free of dipolar fields.

Divide a nanostructure in two or more parts, apply the construction to each of them before bringing all parts back together: a higher order ground state is found with zero dipolar energy. An infinity of such states exists. In experiments such states may be prepared through special (de)magnetization procedures. High order states may also not be stable in a real sample, because the wall width and energy neglected in the model will become prohibitively large. Notice also that the construction may still be used in the case of a weak in-plane magnetic anisotropy in the sample, however suitably dividing the sample in several parts with lines parallel to the easy axis of magnetization (Figure II.11)c.

4.2 Domains in nanostructures with out-of-plane magnetization

Although to a lesser extent than for in-plane magnetization, domains of perpendicularly-magnetized material are influence by lateral finite-size effects. This is obviously the case for weak-stripe domains, as a significant part of magnetization lies in-the-plane, calling for effects similar to those highlighted in the previous paragraph. Strong stripe domains may also be influenced in a flat nanostructure. Two arguments may be put forward: the local demagnetizing field is smaller close to an edge, with respect to the core of a nanostructure; this would favor uniform magnetization close to an edge, and thus local alignement of the stripes along this edge. Another argument is that a stripe with opposite magnetization is 'missing' beyond the border, removing a stabilizing effect on the stripe at the border; this would call for orienting stripes perpendicular to the border to better compensate surface charges. It seems that in some experiments the stripes display a tendency to align either parallel or perpendicular to the border, in the same sample[53]. For thick films it seems that alignement of the stripes parallel to the border is favored[54].

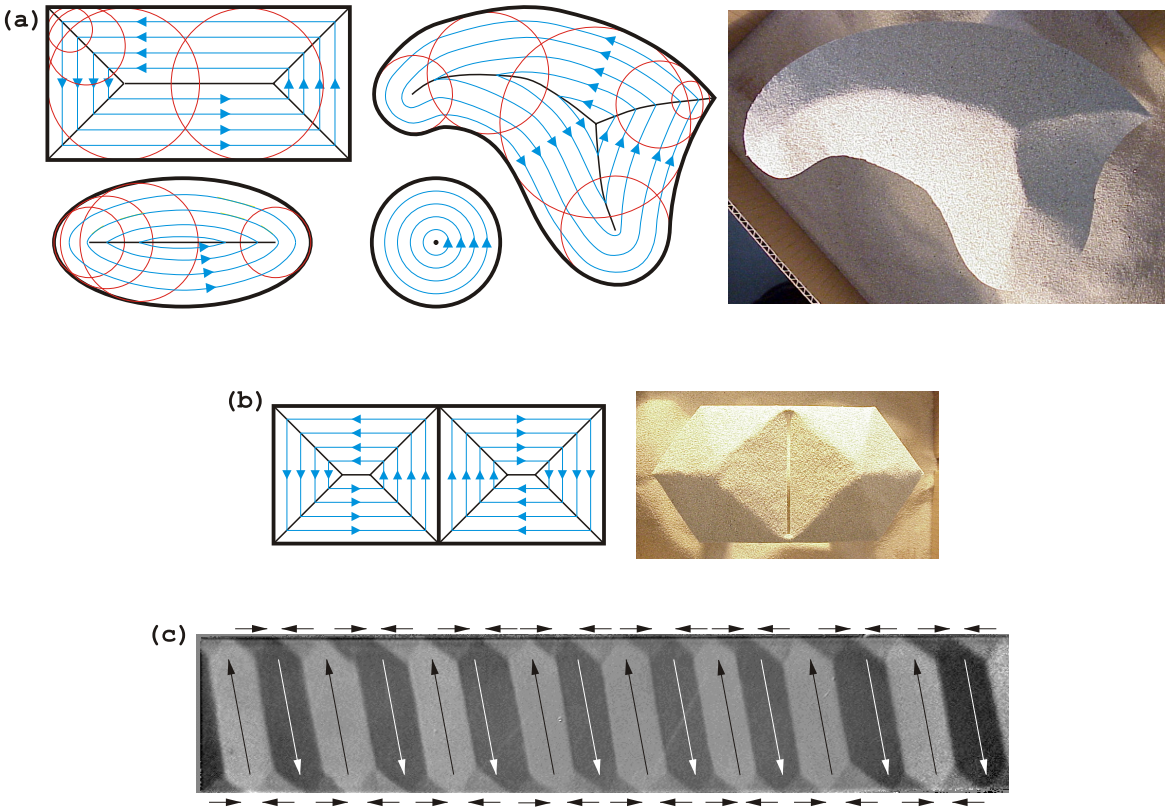

Figure II.11: The geometrical construction of Van den Berg. (a) first order construction, along with a sand pile analogue (b) higher-order construction, along with a sand pile analogue (c) Kerr microscopy of an experimental realization of a high order pattern from a stripe with an in-plane axis of anisotropy (sample courtesy: B. Viala, CEA-LETI).

4.3 The critical single-domain size

In the above we considered domains in large samples. We now examine down to which size domains may be expected in nanostructures, called the critical single-domain size.

Let us consider a rather compact nanostructure, *i.e.* with all three demagnetizing coefficient N close to 1/3, and lateral size l. If uniformly magnetized, its total energy is $\mathcal{E}_{\rm SD} = NK_{\rm d}\,\frac{4}{3}\pi R^3$. We now have to discuss separately the cases of hard versus soft magnetic materials.

In hard magnetic materials domain walls are narrow and with an areal energy density $\gamma_{\rm W}$ determined from materials properties. If split in two domains to close its magnetic flux, the energy of such a nanostructure is $\mathcal{E}_{\rm D} \approx \epsilon_{\rm d} NK_{\rm d} + l^2\gamma_{\rm W}$ with $\epsilon_{\rm D}$ expressing the residual dipolar energy remaining despite the flux closure. $\gamma_{\rm W} = 4\sqrt{AK_{\rm u}}$ in the case of uniaxial anisotropy. Equating $\mathcal{E}_{\rm SD}$ and $\mathcal{E}_{\rm D}$ yields the critical single-domain size $l_{\rm SD} = \gamma_{\rm W}/[N(1-\epsilon_{\rm d})K_{\rm d}]$ below which the single-domain state is expected, while above which splitting into two or more domains is expected. $l_{\rm SD} \approx \gamma_{\rm W}/NK_{\rm d} \approx \sqrt{AK_{\rm u}}/K_{\rm d}$. $l_{\rm SD}$ is of the order of one hundred nanometers for permanent magnet materials.

In soft magnetic materials a flux-closure state often takes the form of a collective magnetization distribution, implying a slow rotation of magnetization as seen in Van

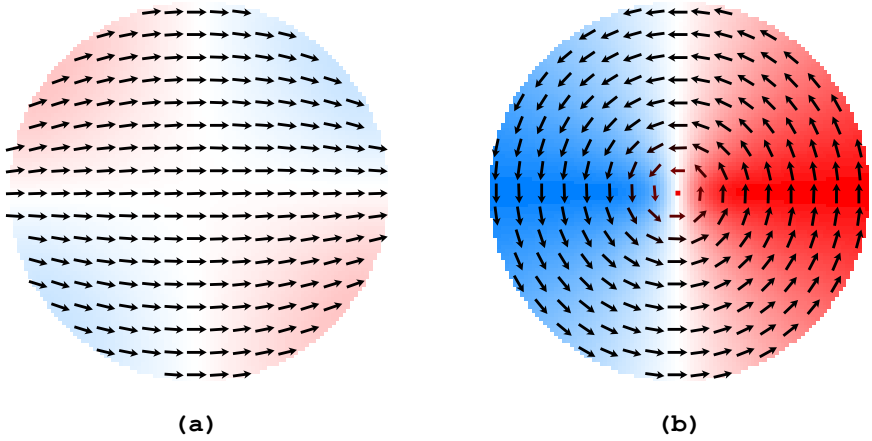

Figure II.12: Magnetization states of a disk of permalloy with diameter 100 nm and thickness 10 nm. The background color codes the y component of magnetization. Arrows stand for the magnetization vector. (a) near single-domain and (b) vortex states.

den Berg's constructions (sec.4.1). The relevant quantities are then exchange and dipolar energy, so that the critical single-domain size is expected to scale with the dipolar exchange length Δ_d. Numerical simulation provides the numerical factor, $l_{SD} \approx 7\Delta_d$ for cubes and $l_{SD} \approx 4\Delta_d$ for spheres[6, p.156].

Estimating the critical single domain dimensions for non-compact nanostructures (*i.e.* with lengths quite different along the three directions) requires specific models. An important case is the transition from single-domain to the vortex state in a disk of diameter w and thickness t (Figure II.12). $\mathcal{E}_{SD} \approx NK_d tw^2$ with $N \approx t/w$ the in-plane demagnetizing coefficient. As a crude estimate the (lower bound for the) energy $\mathcal{E}_D$ of the flux-closure state is the exchange plus dipolar energy of the core, round $10\Delta_d^2 tK_d$. Equating both we find the scaling law $wt \approx 10\Delta_d^2$ for the critical dimensions. Numerical simulation provides an excellent agreement with the scaling law, however refines the numerics: $wt \approx 20\Delta_d^2$[55].

4.4 Near-single-domain

In the previous paragraph we discussed the scaling laws for dimensions, below which a nanostructure does not display domains. Here we notice that such nanostructures are often not perfectly uniformly-magnetized. We discuss the origins and the consequences of this effect.

When deriving the theory of demagnetization coefficients in sec.4.3, we noticed that the self-consistence of the hypothesis of uniform magnetization may be satisfied only in the case of homogenous internal field. In turn, this may be achieved only in ellipsoids, infinite cylinders with elliptical cross-section, and slabs with infinite lateral dimensions. Many samples do not display such shapes, in particular flat structures made by combining deposition and lithography. Figure II.13 shows the demagnetizing field in a flat stripe assumed magnetized uniformly across its width. The field is highly non-homogeneous, being very intense close to the edges (mathematically, going towards $M_s/2$, and very weak in the center, below its average value

$-NM_s$[II.5]. This is a practical example of the statement found in sec.2.1, about the short range of dipolar fields for a two-dimensional nanostructure.

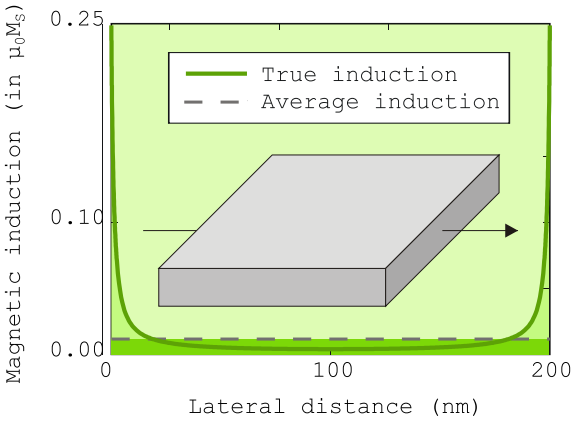

Figure II.13: Demagnetizing field in a stripe magnetized uniformly across the width, of width 200 nm and thickness 2.5 nm

Due to the high value of demagnetizing field close to the edges, magnetization undergoes a strong torque and cannot remain uniformly magnetized, at least in the absence of an external field. The resulting areas are called end domains, with a tendency of magnetization to turn parallel to the edge to reduce edges charges and instead spread them in the volume. Although no real domains develop, this is a reminiscence of the Van den Berg construction. In the case of elongated elements, so-called 'S' and 'C' states arise, named after the shape of the flux lines, and reflecting the mostly independence of end domain when sufficiently apart one from another (Figure II.14a-b).

Non-uniform magnetization configurations may persist down to very small size, especially close to corners where demagnetizing fields diverge in the mathematical limit[56, 57]. This leads to the phenomenon of configurational anisotropy, described both analytically and computationnally[58, 59, 60]: certain directions for the average moment have an energy lower than others, arising from the orientation-dependant decrease of dipolar energy (at the expense of exchange) made possible by the non-uniformity of magnetization. This effect adds up to the quadratic demagnetizing tensor, and may display symmetries forbidden by the latter, in relation with the shape of the element: order 3, 4, 5 etc (Figure II.14c-d). In sec.4.1 we will refer to a method to evaluate experimentally the strength of this anisotropy.

4.5 Domain walls in stripes and wires

We consider nanostructures elongated in one direction, which we will call wires when the sample dimensions are similar along the other two directions, and stripes when one of them is much smaller than the other. The latter is the case for most samples made by lithography, while the former is the case for samples made *e.g.* by electrodeposition in cylindrical pores[61]. We restrict the discussion to those stripes and wires where no magnetocrystalline anisotropy is present, so that shape anisotropy forces magnetization to lie along the axis. Domain walls may be found in long objects, called head-to-head or tail-to-tail depending on the orientation of magnetization in the two segments.

Micromagnetic simulation predicts the existence of two main types of domain walls for stripes: either the vortex wall (VW) or the transverse wall (TW) (Figure II.15). The lowest energy is for the latter for $tw < 61\Delta_d^2$, while the vortex domain wall prevails at large thickness or width. Although this scaling law is simi-

[II.5]The analytical derivation of which is proposed in a problem

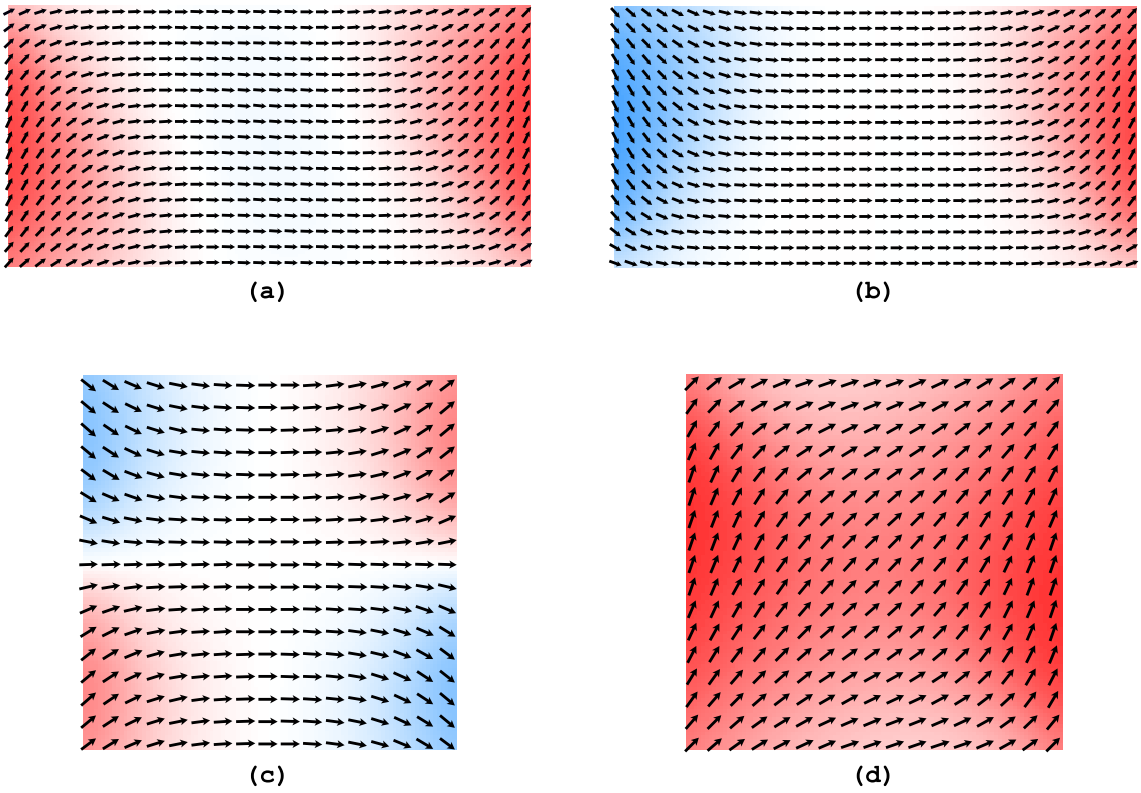

Figure II.14: Near-single-domain state in rectangles of dimensions $200 \times 100 \times 10\,\mathrm{nm}$ and squares of dimensions $100 \times 100 \times 10\,\mathrm{nm}$. (a) S state (b) C state (c) flower state (d) leaf state.

lar to that of the single-domain-versus-vortex phase diagram for disks however with a larger coefficient (sec.4.3), its ground is slightly different. It was indeed noticed that most of the energy in both the VW and TV are of dipolar origin[62], resulting from charges of the head-to-head or tail-to-tail. These charges are spread over the entire volume of the domain wall. Using integration of H_d^2 over space to estimate dipolar energy, and noticing that the surface of the TW is roughly twice as large as that of the VW and the decay with height of H_d is roughly w, the tw scaling law is again derived. Although both transverse and vortex domain walls are observed experimentally, the range of metastability is large so that it is not possible to derive an experimental energetic phase diagram. TW may for instance be prepared far in the metastability area through preparation with a magnetic field transverse to the stripe. For the largest thickness and especially width TW turn asymmetric (ATW) through a second-order transition.

5 An overview of characteristic quantities

In the course of this chapter we met many characteristic quantities: lengths, energies, dimensionless ratios etc. Here we make a short summary of them.

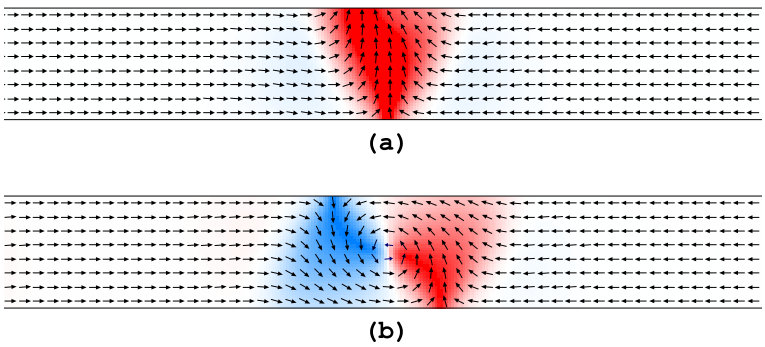

Figure II.15: Head-to-head domain walls in stripes, of (a) transverse and (b) vortex type.

5.1 Energy scales

- $K_\mathrm{d} = (1/2)\mu_0 M_\mathrm{s}^2$ is called the dipolar constant. It is a measure of the maximum dnsity of dipolar energy that can arise in a volume, *i.e.* for demagnetizing coefficient $N = 1$.

- $4\sqrt{AK_\mathrm{u}}$ is the energy of a Bloch wall per unit area.

5.2 Length scales

- In a situation where only magnetic exchange and anisotropy compete, the two relevant quantities in energy are A and K_u, expressed respectively in J/m and J/m^3. The typical case is that of a Bloch domain wall (sec.5). The resulting length scale is $\Delta_\mathrm{u} = \sqrt{A/K_\mathrm{u}}$. We call Δ_u the anisotropy exchange length[10] or Bloch parameter, a name often found in the literature. The latter is more often used, however the former makes more sense, see the note below. Notice that Δ_u is sometimes called the Bloch wall width, which however brings some confusion as several definitions may be used for this, see sec.6.5.c.

- When exchange and dipolar energy compete, the two quantities at play are A and K_d. This the case in the vortex (sec.3.4). The resulting length scale is $\Delta_\mathrm{d} = \sqrt{A/K_\mathrm{d}} = \sqrt{2A/\mu_0 M_\mathrm{s}^2}$, which we call dipolar exchange length[6] or exchange length as more often found in the literature, see again the note below.

- $l_\mathrm{SD} \approx \sqrt{AK_\mathrm{u}}/K_\mathrm{d}$ is the critical domain size of a compact nanostructure made of a quite hard magnetic material. It emerges out of the comparison of two energies, one per unit volume, the other one per unit surface.

- In more complex situations other length scales may arise, taking into account an applied magnetic field, dimensionless quantities such as the ratio of geometric features etc. For example the pinning of a domain wall on a defect gives rise to the length scale $\sqrt{A/\mu_0 M_\mathrm{s} H}$ for a soft magnetic material, or $\sqrt{2A/\sqrt{K_\mathrm{u}\mu_0 M_\mathrm{s} H}}$ for a material with significant magnetic anisotropy.

The name exchange length has historical grounds however is not well suited. Indeed exchange plays an equal role in both Δ_u and Δ_d. It is more relevant to name Δ_u the anisotropy length or anisotropy exchange length, and Δ_d the dipolar length or dipolar exchange length. We use the subscripts u (for uniaxial) and d (for dipolar) to account for this, as suggested in Hubert's book[6].

5.3 Dimensionless ratios

- A quantity of interest in the quality factor $Q = K_u/K_d$, which describes the competition between uniaxial anisotropy and dipolar energy. Q largely determines the occurrence and type of domains in thin films with an out-of-plane magnetocrystalline anisotropy.

Problems for Chapter II

Problem 1: Short exercises

1. Consider a cubic material with first-order magnetocrystalline anisotropy constant $K_{1,\mathrm{cub}}$ much weaker than K_d, in the form of a thin film with surface normal (001).

   - Express the resulting in-plane magnetic anisotropy $E(\theta)$ with θ the in-plane angle of magnetization with an easy axis, assuming that magnetization lies purely in-the-plane. Comment.
   - Find exactly the easy directions of magnetization.

   For both items consider both cases of positive and negative $K_{1,\mathrm{cub}}$, and comment.

2. Draw a sketch of the expected contrast in the magnetic microscopy of domain walls. Consider four types of domain walls: perpendicular anisotropy with Bloch wall; in-plane anisotropy with Bloch wall and Néel caps, 180° Néel wall and 180° Néel wall. Consider four techniques: XMCD-PEEM, Lorentz, MFM, polar Kerr. The sketches may be presented as an array for clarity.

3. Derive with simple arguments the scaling law $W \sim t^{1/2}$ for the period of strong stripe domains.

Problem 2: Demagnetizing field in a stripe

Here we derive the analytical formula for the in-plane demagnetizing field in a flat and infinitely-long stripe magnetized in-the-plane, a case that was shortly discussed in sec.4.4. We call t and w its thickness and width, respectively. We assume magnetization to be homogeneous and along the transverse direction.

2.1. Deriving the field

Express the stray field H_d arising from a line holding the magnetic charge per unit length λ. As a first step, we consider only $H_{\mathrm{d},x}(x)$, the x component of the demagnetizing field calculated at mid-height of the stripe, arising from the charges

on one of its edges. Write an integral form for this function. Show that it reads, upon integration:

$$H_{\mathrm{d},x}(x) = \frac{M_\mathrm{s}}{2}\left[1 - \frac{2}{\pi}\arctan\left(\frac{2x}{t}\right)\right] \tag{II.11}$$

2.2. Numerical evaluation and plotting

Derive the limits and first derivative for Eq. (II.11) for $x \to 0$ and $x \to \infty$, and comment. Provide a hand-drawn qualitative plot of this function. Without performing more calculation, discuss how it compares in magnitude with the z average over the thickness, *i.e.* $\langle H_{\mathrm{d},x,z}\rangle\,(x)$? What is the (x, z) average of the latter over the entire cross-section of the stripe?

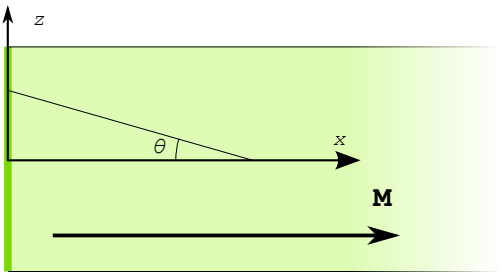

Figure II.16: Left part of the stripe considered. The edge holding the magnetic charges is highlighted as a bold line. Magnetization is along x, while a translation invariance is assumed along y.

Chapter III

Magnetization reversal

1 Coherent rotation of magnetization

Overview

The importance of metastability in magnetism was outlined in 1.3, as the reason for hysteresis. The determination of energy minima, landscape and energy barriers is therefore crucial, however difficult or impossible in extended systems due to the large number of degrees of freedom. Only simple problems can be tackled analytically. Coherent rotation of magnetization is one of the oldest and probably the most useful starting point.

1.1 The Stoner-Wohlfarth model

The model of coherent rotation was proposed by Stoner and Wohlfarth in 1948 to describe the two-dimensional angular dependance of magnetization reversal[63, 64, reprint], and developed in parallel by Néel to describe thermally-activated processes. Many developments were made later, including clever graphical interpretations[65]and generalization to three dimensions[66].

The model is based on the hypothesis of uniform magnetization, reducing the problem to solely one or two angular degrees of freedom. This hypothesis is in principle very restrictive and would be satisfactorily applicable to closely single-domain particles. For large systems it is not suitable as it, with for example an experimental coercivity much smaller than the one predicted. Nevertheless, the concept introduced for uniform magnetization bear some generality (*e.g.* exponents, angular dependance), and may be applied to extended systems with some care, *e.g.* to describe nucleation volumes.

We consider a system with volume V, total uniaxial anisotropy energy $\kappa = K_\mathrm{u}V$, magnetic moment $\mathcal{M} = M_\mathrm{s}V$. Its magnetic energy reads:

$$\mathcal{E} = \kappa \sin^2\theta - \mu_0 \mathcal{M} H \cos(\theta - \theta_H) \tag{III.1}$$

where θ_H is the angle between the applied field and the easy axis and initial direction of magnetization, and H is positive to promote magnetization reversal. Here we consider only the usual case of $\theta_H = \pi$, and use dimensionless variable:

$$e = E/\kappa = \sin^2\theta + 2h\cos\theta \tag{III.2}$$

with $H_a = 2K/\mu_0 M_s$ and $h = H/H_a$. The equilibrium positions are determined by solving $d_\theta e = 2\sin\theta(\cos\theta - h) = 0$, and stability with the sign of $d^2_{e^2}\theta = 4\cos^2\theta - 2h\cos\theta - 2$.

Pour $h < 1$ les positions d'équilibre sont donc $\theta_1^+ = 0$, $\theta_1^- = \pi$ et θ_2 tel que $\cos\theta_2 = h$. Pour ces angles la dérivée seconde vaut $2(1-h)$, $2(1+h)$ et $2(1-h^2)$, respectivement. $\theta_1^\pm$ sont donc des positions d'équilibre stables, et $\theta_2^\pm = \pm\arccos(h)$ est une position d'équilibre instable, qui marque le sommet de la barrière d'énergie qui empêche le renversement d'aimantation de θ_1^+ vers θ_1^-. Pour $h > 1$ il n'existe plus que θ_1^- et θ_1^+ comme points d'équilibre, respectivement stable et instable. Le retournement d'aimantation a donc lieu à $h = 1$.

1.2 Dynamic coercivity and temperature effects

2 Magnetization reversal in nanostructures

2.1 Multidomains under field (soft materials)

2.2 Nearly single domains

2.3 Domain walls and vortices

3 Magnetization reversal in extended systems

3.1 Nucleation and propagation

3.2 Ensembles of grains

Some features of the magnetization reversal of isolated single-domain grains have been presented in sec.1. Some consequences may be drawn for media consisting of assemblies of grains, neglecting inter-grain interactions (dipolar etc). Of easy access and modeling are the remanence m_r and the internal energy at saturation E_K, derived from the area above the remagnetizing curve (*i.e.*, starting from remanence, see sec.chap.I.1.3 and later sec.4.1). Both depend on the dimensionality of the distribution of easy axis. Assuming uniaxial magnetic anisotropy for simplicity, we consider three common cases:

- The polycrystalline case, *i.e.* with an isotropic distribution of easy axis in space. This may correspond to particles diluted in a matrix, or a polycristalline bulk material. We then find: $m_r^{3D} = 1/2$ and $E_K^{3D} = 2K/3$.
- The polytextured case. By this we mean a shared axis with no distribution for the hard axis, while the easy axis if evenly distributed in the plane perpendicular to this axis. This would be the case of Fe(110) grains grown on a surface, the easy axis lying along the in-plane [001] direction. When the field is applied in the plane we find: $m_r^{2D} = 2/\pi \approx 0.64$ and $E_K^{2D} = K/2$.
- The textured case, where all grains share the same direction of easy axis. When the field is applied along this axis we find the case of a single grain: $m_r^{1D} = 1$ and $E_K^{1D} = 0$.

The measure of E_K provides an indication of K. Besides, comparison of experiments with the expected figure for m_r is often used as an indication for interactions, positive (*e.g.* through direct exchange between neighboring grains) if the experimental value exceeds the expectation, negative it it lies below. Systems with coupled grains will be considered in more detail in chap.V.

4 What do we learn from hysteresis loops?

4.1 Magnetic anisotropy

Measure total anisotropy. Notice/reminder: area above curve. Linear for uniaxial, other shapes with possibly hysteresis, Cf (110), (001). Trick for these: loops under transverse field. Show angular curves for anisotropy.

4.2 Nucleation versus propagation

First magnetization curves: nucleation versus propagation
Hc(theta), Kondorski

4.3 Distribution and interactions

Minor loops: reversible versus irreversible; hints for interactions.
Interactions: Henkel plots.
Complex: Preisach, now often called FORC.

Problems for Chapter III

Problem 1: Short exercises

1. Give a realistic example of a magnetically-uniaxial system whose coercivity H_c is larger than its anisotropy field H_a.

2. Derive the formulas for remanence m_r and remagnetization energy E_K for the various cases of texture provided in sec.3.2.

Problem 2: A model of pinning - Kondorski's law for coercivity

We consider a one-dimensional framework, identical to the one used to derive the profile of the Bloch domain wall, see pb. 6.5.c. Starting from a homogeneous material let us model a local defect in the form of a magnetically softer (*i.e.* anisotropy constant $K-\Delta K$ with $\Delta K > 0$) insertion of width $\delta\ell$, located at position x. Discuss what approach should be followed to derive exactly the profile of the domain wall in that case, especially the boundary conditions at the edges of the defect. To handle simple algebra we make the assumption of the rigid domain wall, *i.e.* Eq. (I.37) still holds, and consider the case where $\delta\ell \ll \Delta$.

Show that the energy of the domain wall with the defect at location x reads:

$$E(x) = 4\sqrt{AK}\left[1 - \frac{1}{4}\frac{\delta\ell}{\Delta}\frac{\delta K}{K}\frac{1}{\cosh^2(x/\Delta)}\right] \tag{III.3}$$

Draw a schematic graph of $E(x)$ and display the characteristic length or energy scales. An external field is then applied at an angle $\cos\theta_H$ with the easy axis direction in the domains. Assuming that the assumption of rigid wall remains valid, show that the propagation field of the domain wall over the defect reads:

$$H_p = \frac{H_a}{\cos\theta_H}\frac{\Delta K}{K}\frac{\delta\ell}{\Delta}\frac{1}{3\sqrt{3}}. \tag{III.4}$$

where $H_a = 2K/\mu_0 M_s$ is the so-called anisotropy field.
Notice:

- The $1/\cos\theta_{\mathrm{H}}$ dependence of coercivity is often considered as a signature a weak-pinning mechanism, a law known as the Kondorski model[67].
- This model had been initially published in 1939 by Becker and Döring[68], and is summarized *e.g.* in the nice book of Skomsky *Simple models of Magnetism*[5].
- While coercivity requires a high anisotropy, the latter is not a sufficient condition to have a high coercivity. To achieve this one must prevent magnetization reversal that can be initiated on defects (structural or geometric) and switch the entire magnetization by propagation of a domain wall. In a short-hand classification one distinguishes coercivity made possible by hindering nucleation, or hindering the propagation of domain walls. In reality both phenomena are often intermixed. Here we modeled an example of pinning.
- Simple micromagnetic models of nucleation on defects[69] were the first to be exhibited to tentatively explain the so-called *Brown paradox*, *i.e.* the fact that values of experimental values of coercivity in most samples are smaller or much smaller than the values predicted by the ideal model of coherent rotation[63].

Chapter IV

Precessional dynamics of magnetization

Problems for Chapter IV

Chapter V

Magnetic heterostructures: from specific properties to applications

Problems for Chapter V

Appendices

Symbols

K_d	Dipolar anisotropy	$K_\mathrm{s} = \frac{1}{2}\mu_0 M_\mathrm{s}^2$
Q	Quality factor	$Q = K_\mathrm{mc}/K_\mathrm{d}$
Δ_u	Anisotropy exchange length	$\Delta = \sqrt{A/K}$ with A the exchange and K the anisotropy constant. Also called: Bloch wall parameter
Δ_d	Dipolar exchange length	$\Lambda = \sqrt{A/K_\mathrm{d}} = \sqrt{2A/\mu_0 M_\mathrm{s}^2}$ with A the exchange and M_s the spontaneous magnetization. Also called: exchange length.

Acronyms

AFM	Atomic Force Microscopy
EMF	Electromotive force
MFM	Magnetic Force Microscopy
PMA	Perpendicular Magnetic Anisotropy
SEMPA	Scanning Electron Microscopy with Polarization Analysis (SEMPA)
SPLEEM	Spin-Polarized Low-Energy Electron Microscopy
SQUID	Superconducting Quantum Interference Device
UHV	Ultra-High Vacuum
VSM	Vibrating Sample Magnetometer

Glossary

erg	Unit for energy in the cgs-Gauss system. Is equivalent to 10^{10} J.
Macrospin	The model where uniform magnetization is assumed in a system, whose description may thus be restricted to the knowledge of one or two degrees of freedom, the angular directions of a hypothetical spin. When formerly written as a variable, the macrospin may be dimensionless, or have units of A.m^2 for a volume, A.m for magnetization integrated over a surface (*e.g.* that of a nanowire), or A for magnetization integrated along a thickness (*e.g.* that of a thin film).
Micromagnetism	All aspects related the arrangement of magnetization in domains and domain walls, when the latter are resolved (*i.e.*, not treated as a plane with zero thickness nor energy). The term applies to theory, simulation and experiments. Except some rare cases that may be considered as fine points, micromagnetism is based on the description of magnetization by a continuous function of constant and homogeneous magnitude equal to the spontaneous magnetization M_s.
Nanomagnetism	Broadly speaking, all aspects of magnetism at small length scale, typically below one micrometer. This concerns ground-state (intrinsic) properties such as magnetic ordering and magnetic anisotropy, as well as magnetization configurations and magnetization reversal at these small scales. Notice that some persons restrict the meaning of Nanomagnetism to the former

Bibliography

[1] S. Blundell, Magnetism in condensed matter, Oxford University Press, 2001, a basic however clear and precise review of magnetism in condensed matter. Definitely a major reference. 7, 15

[2] R. Skomski, Simple models of magnetism, Oxford, 2008, an excellent entry point for magnetism, especially nanomagnetism. Simple and handwavy presentations, with references for readers seeking a deeper insight. 7

[3] J. M. D. Coey, Magnetism and magnetic materials, Cambride University Press, 2010, an excellent book about magnetism. Of particular interest for reviewing properties of various types of materials and compounds. To read absolutely. 7, 15

[4] C. L. Dennis, R. P. Borges, L. D. Buda, U. Ebels, J. F. Gregg, M. Hehn, E. Jouguelet, K. Ounadjela, I. Petej, I. L. Prejbeanu, M. J. Thornton, The defining length scales of mesomagnetism: a review, J. Phys.: Condens. Matter 14, R1175–R1262 (2002). 7

[5] R. Skomski, Nanomagnetics, J. Phys.: Condens. Matter 15, R841–896 (2003), review: overview of fundamental and micromagnetic aspects (static and dynamic) of growth and artificial magnetic nanostructures. 7, 68

[6] A. Hubert, R. Schfer, Magnetic domains. The analysis of magnetic microstructures, Springer, Berlin, 1999, micromagnetic theories and experimental results, imaging techniques. 7, 21, 24, 28, 29, 51, 52, 53, 54, 57, 60, 61

[7] A. P. Guimaraes, Principles of Nanomagnetism, Springer, 2009. 7

[8] F. Cardarelli, Scientific units, weights and measures, Springer, Berlin, 2003, comprehensive reference about units: systems, conversions, and incredible set of units in all fields of physics and beyond. 15

[9] J. Sthr, H. C. Siegmann, Magnetism – From fundamentals to nanoscale dynamics, no. 152 in Springer series in Solid-State Sciences, Springer, Heidelberg, 2006, comprehensive review book on Magnetism. Slightly annoying with respect to the choice of defining $\mathbf{B} = \mu_0\mathbf{H} + \mathbf{M}$. 17

[10] A. HUBERT, W. RAVE, Systematic Analysis of Micromagnetic Switching Processes, Phys. Stat. Sol. (b) 211 (2), S815–829 (1999). 21, 60

[11] E. C. STONER, Philos. Mag. 36, 803 (1945). 24

[12] P. RHODES, G. ROWLANDS, Demagnetizing energies of uniformly magnetized rectangular blocks, Proc. Leeds Phil. Liter. Soc. 6, 191 (1954), `demagnetizing factor in rectangular blocks`. 24

[13] A. AHARONI, Demagnetizing factors for rectangular ferromagnetic prisms, J. Appl. Phys. 83 (6), 3432–3434 (1998). 24

[14] G. ROWLANDS, Ph.D. thesis, University of Leeds, Leeds (1956). 24

[15] P. RHODES, G. ROWLANDS, D. R. BIRCHALL, J. Phys. Soc. Jap. 17, 543 (1956). 24

[16] D. A. GOODE, G. ROWLANDS, The demagnetizing energies of a uniformly magnetized cylinder with an elliptic cross-section, J. Magn. Magn. Mater. 267, 373–385 (2003). 24

[17] G. ROWLANDS, On the calculation of acoustic radiation impedance of polygonal-shaped apertures, J. Acoust. Soc. Am. 92 (5), 2961–2963 (1992). 24

[18] M. BELEGGIA, M. DE GRAEF, On the computation of the demagnetization tensor field for an arbitrary particle shape using a Fourier space approach, J. Magn. Magn. Mater. 263, L1–9 (2003). 24

[19] J. C. MAXWELL, in: A Treatise on Electricity and Magnetism, 3rd Edition, Vol. 2, Clarendon, Oxford, 1872, pp. 66–73. 24

[20] B. A. LILLEY, Energies and widths of domain boundaries in ferromagnetics, Philos. Mag. 41 (7), 401–406 (1950). 29

[21] Y. ZHU (Ed.), Modern techniques for characterizing magnetic materials, Springer, Berlin, 2005, `covers many characterization techniques, including microscopies.` 29, 30

[22] H. HOPSTER, H. P. OEPEN (Eds.), Magnetic Microscopy of Nanostructures, Springer, 2005. 29, 30

[23] H. KRONMLLER, S. S. P. PARKIN (Eds.), Handbook of magnetism and advanced magnetic materials, Wiley, 2007, `several thousands of pages of review articles dedicated to many topics in Magnetism. Always to be checked when you search for something.` 29

[24] P. EATON, P. WEST, Atomic force microscopy, Oxford, 2010. 30

[25] F. BLOCH, Z. Phys. 74, 295 (1932). 35

[26] G. A. T. ALLAN, Critical temperatures of Ising Lattice Films, Phys. Rev. B 1 (1), 352–357 (1970). 40

[27] U. GRADMANN, Magnetism in ultrathin transition metal films, in: K. H. J. BUSCHOW (Ed.), Handbook of magnetic materials, Vol. 7, Elsevier Science Publishers B. V., North Holland, 1993, Ch. 1, pp. 1–96, `review: Magnetic fundamental properties in continuous thin films: methods, magnetic anisotropy, temperature dependance of magnetization, ground state properties (interface magnetization), metastable phases`. 40, 41, 44

[28] L. ONSAGER, Crystal Statistics. I. A Two-Dimensional Model with an Order-Disorder Transition, Phys. Rev. 65, 117–149 (1944). 40

[29] H. E. STANLEY, T. A. KAPLAN, Phys. Rev. Lett. 17, 913 (1966). 40

[30] M. BANDER, D. I. MILLS, Phys. Rev. B 43, 11527 (1988). 40

[31] P. GAMBARDELLA, A. DALLMEYER, K. MAITI, M. C. MALAGOLI, W. EBERHARDT, K. KERN, C. CARBONE, Ferromagnetism in one-dimensional monoatomic metal chains, Nature 416, 301–304 (2002). 41

[32] J. BANSMANN, S. BAKER, C. BINNS, J. BLACKMAN, J.-P. BUCHER, J. DORANTES-DVILA, V. DUPUIS, L. FAVRE, D. KECHRAKOS, A. KLEIBERT, K.-H. MEIWES-BROER, G. M. PASTOR, A. PEREZ, O. TOULEMONDE, K. N. TROHIDOU, J. TUAILLON, Y. XIE, Magnetic and structural properties of isolated and assembled clusters, Surf. Sci. Rep. 56, 189–275 (2005), `review of a European project on the subject, mainly focused on clusters`. 41

[33] A. J. COX, J. G. LOUDERBACK, L. A. BLOOMFIELD, Experimental observation of magnetism in rhodium clusters, Phys. Rev. Lett. 71 (6), 923–926 (1993). 41

[34] A. J. COX, J. G. LOUDERBACK, S. E. APSEL, L. A. BLOOMFIELD, Magnetism in 4d-transition metal clusters, Phys. Rev. B 49 (17), 12295–12298 (1994). 41

[35] U. GRADMANN, J. MLLER, Flat ferromagnetic exitaxial 48Ni/52Fe(111) films of few atomic layers, Phys. Stat. Sol. 27, 313 (1968). 45

[36] M. T. JOHNSON, P. J. H. BLOEMEN, F. J. A. DEN BROEDER, J. J. DE VRIES, Magnetic anisotropy in metallic multilayers, Rep. Prog. Phys. 59, 1409–1458 (1996). 44, 45

[37] M. DUMM, B. UHL, M. ZLFL, W. KIPFERL, G. BAYREUTHER, Volume and interface magnetic anisotropy of $Fe_{1-x}Co_x$ thin films on GaAs(001), J. Appl. Phys. 91 (10), 8763 (2002). 45

[38] D. T. D. LACHEISSERIE, Magnetostriction - Theory and Applications of Magnetoelasticity, CRC Press, 1993. 46

[39] W. A. JESSER, D. KUHLMANN-WILSDORF, On the theory of interfacial energy and elastic strain of epitaxial overgrowth in parallel alignment on single crystal substrates, Phys. Stat. Sol. 19 (1), 95–105 (1967), `first model for` $1/t$ `strain relaxation in thin films related to misfit dislocations`. 46

[40] C. CHAPPERT, P. BRUNO, Magnetic anisotropy in metallic ultrathin films and related experiments on cobalt films, J. Appl. Phys. 64 (10), 5336–5341 (1988), `first application of the theory of strain relaxation in thin films to the ambiguity if interface and magnetoelastic anisotropy`. 46

[41] D. SANDER, R. SKOMSKI, A. ENDERS, C. SCHMIDTHALS, D. REUTER, J. KIRSCHNER, The correlation between mechanical stress and magnetic properties of ultrathin films, J. Phys. D: Appl. Phys. 31, 663–670 (1998). 47

[42] C. CHAPPERT, H. BARNAS, J. FERR, V. KOTTLER, J.-P. JAMET, Y. CHEN, E. CAMBRIL, T. DEVOLDER, F. ROUSSEAUX, V. MATHET, H. LAUNOIS, Planar patterned magnetic media obtained by ion irradiation, Science 280, 1919–1922 (1998). 47

[43] L. NEL, nergie des parois de Bloch dans les couches minces, C. R. Acad. Sci. 241 (6), 533–536 (1955). 48

[44] K. RAMSTCK, W. HARTUNG, A. HUBERT, The phase diagram of domain walls in narrow magnetic strips, Phys. Stat. Sol. (a) 155, 505 (1996). 48, 49

[45] A. E. LABONTE, Two-dimensional Bloch-type domain walls in ferromagnetic thin films, J. Appl. Phys. 40 (6), 2450–2458 (1969). 48, 49

[46] A. HUBERT, Stray-field-free magnetization configurations, Phys. Stat. Sol. 32 (519), 519–534 (1969). 48

[47] S. FOSS, R. PROKSCH, E. DAHLBERG, B. MOSKOWITZ, B. WALSCH, Localized micromagnetic perturbation of domain walls in magnetite using a magnetic force microscope, Appl. Phys. Lett. 69 (22), 3426–3428 (1996). 49

[48] H. JOISTEN, S. LAGNIER, M. VAUDAINE, L. VIEUX-ROCHAZ, J. PORTESEIL, A magnetic force microscopy and Kerr effect study of magnetic domains and cross-tie walls in magnetoresistive NiFe shapes, J. Magn. Magn. Mater. 233, 230 (2001). 51

[49] W. DRING, Point singularities in micromagnetism, J. Appl. Phys. 39 (2), 1006 (1968). 52

[50] C. KITTEL, Physical theory of ferromagnetic domains, Rev. Mod. Phys. 21 (4), 541–583 (1949). 52

[51] H. A. M. VAN DEN BERG, A micromagnetic approach to the constitutive equation of soft-ferromagnetic media, J. Magn. Magn. Mater. 44 (1-2), 207–215 (1984). 54

[52] H. A. M. VAN DEN BERG, Self-consistent domain theory in soft-ferromagnetic media. II. Basic domain structures in thin-film objects, J. Appl. Phys. 60, 1104 (1986). 54

[53] R. DANNEAU, P. WARIN, J. P. ATTAN, I. PETEJ, C. BEIGN, C. FERMON, O. KLEIN, A. MARTY, F. OTT, Y. SAMSON, M. VIRET, Individual Domain Wall Resistance in Submicron Ferromagnetic Structures, Phys. Rev. Lett. 88 (15), 157201 (2002). 55

[54] M. HEHN, K. OUNADJELA, J. P. BUCHER, F. ROUSSEAUX, D. DECANINI, B. BARTENLIAN, C. CHAPPERT, Nanoscale Magnetic Domains in Mesoscopic Magnets, Science 272, 1782–1785 (1996). 55

[55] P. O. JUBERT, R. ALLENSPACH, Analytical approach to the single-domain-to-vortex transition in small magnetic disks, Phys. Rev. B 70, 144402/1–5 (2004). 57

[56] A. THIAVILLE, D. TOMAS, J. MILTAT, On Corner Singularities in Micromagnetics, Phys. Stat. Sol. 170, 125 (1998). 58

[57] W. RAVE, K. RAMSTCK, A. HUBERT, Corners and nucleation in micromagnetics, J. Magn. Magn. Mater. 183, 329–333 (1998). 58

[58] M. A. SCHABES, H. N. BERTRAM, Magnetization processes in ferromagnetic cubes, J. Appl. Phys. 64 (3), 1347–1357 (1988). 58

[59] R. P. COWBURN, M. E. WELLAND, Analytical micromagnetics of near single domain particles, J. Appl. Phys. 86 (2), 1035–1040 (1999). 58

[60] R. DITTRICH, A. THIAVILLE, J. MILTAT, T. SCHREFL, Rigorous micromagnetic computation of configurational anisotropy energies in nanoelements, J. Appl. Phys. 93 (10), 7891–7893 (2003). 58

[61] A. FERT, J. L. PIRAUX, Magnetic nanowires, J. Magn. Magn. Mater. 200, 338–358 (1999). 58

[62] R. MCMICHAEL, M. DONAHUE, Head to Head Domain Wall Structures in Thin Magnetic Strips, IEEE Trans. Magn. 33, 4167 (1997). 59

[63] E. C. STONER, E. P. WOHLFARTH, A Mechanism of Magnetic Hysteresis in Heterogeneous Alloys, Phil. Trans. Roy. Soc. Lond. A 240, 599–642 (1948). 64, 68

[64] E. C. STONER, E. P. WOHLFARTH, reprint of 1948 'A Mechanism of Magnetic Hysteresis in Heterogeneous Alloys', IEEE Trans. Magn. 27 (4), 3469–3518 (1991). 64

[65] J. C. SLONCZEWSKI, Theory of magnetic hysteresis in films and its applications to computers, Research Memo RM 003.111.224, IBM Research Center, Poughkeepsie, NY (1956). 64

[66] A. THIAVILLE, Extensions of the geometric solution of the two dimensional coherent magnetization rotation model, J. Magn. Magn. Mater. 182, 5–18 (1998). 64

[67] E. KONDORSKI, On the nature of coercive force and irreversible changes in magnetisation, Phys. Z. Sowjetunion 11, 597 (1937). 68

[68] R. BECKER, W. DRING, Ferromagnetismus, Springer, 1939, `first model of strong pinning of a Bloch domain will a delta-like defect.` 68

[69] A. AHARONI, Reduction in Coercive Force Caused by a Certain Type of Imperfection, Phys. Rev. 119 (1), 127–131 (1960). 68

[70] B. HAUSMANNS, T. P. KROME, G. DUMPICH, E. WASSERMANN, D. HINZKE, U. NOWAK, K. D. USADEL, Magnetization reversal process in thin Co nanowires, J. Magn. Magn. Mater. 240, 297 (2002). 81

A faire...

Finalisation de poly ED

- F/AF: voir historique et références dans talk Bernard Diény, livre conférences I, p15 (CLN9).
- Citer pour coercitivité SyAF: H. A. M. van den Berg, W. Clemens, G. Gieres, G. Rupp, and M. Vieth, IEEE Trans. Magn. 32, 4624 (1996) (cité dans Wiese 2004).
- courbe FC/ZFC: traiter le cas à une particule (phy stat et susceptibilités première et seconde) puis le cas de distribution. Définition de Tb moyen dans ce cas. Faire le lien avec distribution de champ de renversement, et définition de Hc comme champ de mi-renversement.
- utilisation de hyperref pour les notes de bas de page?
- Noter superparamagnétisme de bandes étroites: LEE2009b.
-
- Nouvel environnement pour:
  - Améliorations
  - Exercices et corrigés
  - Partie difficile (zigzag dans la marge, Cf bouquin Knuth, ou p.76 de symbols-a4.pdf, dbend)
  - Vérifier présence d'introductions et conclusion locales
  - Renversement d'aimantation dans lignes:
    * Hausmanns2002[70]: note que champ coercitif augmente comme $1/w$, mais pas de modèle.
    * BRA2006: cite ceux précédents qui ont noté cette loi d'échelle. Indique également séparation entre nucléation-propagation, et multidomaines (ligne très différente de régime transverse-vortex).
    * Un des premiers modèles: YUA1992
    * Utiliser: Uhlig
  - Interactions dipolaires: Cf études suppression superpara par Cowburn, et changement énergie démagnétisante dans JAI2010.
- Regarder exemples présentations, et chercher code:
  - Thèse Géraud Moulas
  - Thèse Fabien Cheynis
  - Thèse Aurélien Massebœuf (Cf: p.62)

Généralités

- Tableau des matériaux: rajouter:
  - Permalloy (et supermalloy)
  - indiquer échange, longueurs échange et Bloch.
- Changer style de macro lecturePage
- Chercher si package dérivées est défini quelque part.
- Regarder utilisation package vector
- Test page gauche ou droite pour mettre les encadrés et leur image. (utiliser macro: ifodd)
- Redéfinir un environnement enumerate pour les encadrés, pour éviter espace vide en haut. Voir *The tendency to cancel surface magnetic charges* mais en enlevant aussi la marge.
- Changer police de la légende
- Mentionner temps très raccourci entre développement dans laboratoires, et mise en application dans l'industrie. Pour certains secteurs la RD est même plus active que laboratoires fondamentaux, par exemple pour maîtriser les processus de renversement d'aimantation dans les nanostructures.
- Employer Configuration magnétique ou État micromagnétique, et introduire les deux termes. Vérifier dans tout le texte que pas de mélange.
- Normaliser l'usage de termes suivants, pour les renvois:
  - Chapitre
  - Partie
  - Paragraphe
- Mettre un glossaire, et un lien vers le glossaire à chaque fois que le terme est employé (rechercher dans littérature).
- Vérifier présence: différents modes de propagation des ondes de spin, voir cours Hillebrands. Traitement classique et quantique des ODS (exercice?).

Exercices possibles

- Position et valeur du maximum pour le J avec règles de Hund, pour ℓ quelconque. Même chose pour valeur de moment magnétique.